

**AUTOMATED CONSTRUCTION PROGRESS MONITORING
USING RANGE IMAGING**

A THESIS

submitted by

MADHUMITHA SENTHILVEL

for the award of the degree of

MASTER OF SCIENCE

(By Research)



**BUILDING TECHNOLOGY AND CONSTRUCTION MANAGEMENT DIVISION
DEPARTMENT OF CIVIL ENGINEERING
INDIAN INSTITUTE OF TECHNOLOGY MADRAS**

NOVEMBER 2017

THESIS CERTIFICATE

This is to certify that the thesis titled '**AUTOMATED CONSTRUCTION PROGRESS MONITORING USING RANGE IMAGING**', submitted by **Madhumitha Senthilvel**, to the Indian Institute of Technology Madras, for the award of the degree of Master of Science, is a bonafide record of the research work carried out by her under my supervision. The contents of this thesis, in full or in parts, have not been submitted to any other Institute or University for the award of any degree or diploma.

Dr. Koshy Varghese
(Research Guide)
Professor,
Department of Civil Engineering,
Indian Institute of Technology Madras,
Chennai - 600 036

Dr. Ramesh Babu. N
(Research Co-Guide)
Professor,
Department of Mechanical Engineering,
Indian Institute of Technology Madras,
Chennai - 600 036

Chennai, India
11th November, 2017

ACKNOWLEDGEMENT

This thesis marks the end of my M.S journey. It has been a wonderful ride. At this end of my journey, I would like to thank all those who have made this experience an unforgettable one.

I would like to take this opportunity to thank Dr. Koshy Varghese for encouraging me to grow as a researcher. He has been a tremendous influence, both professionally and personally. His advice, visions, network and the discussions helped me expand my horizons. He helped me in defining the roadmap for this study. He has provided many opportunities during my course of study, one of which was introducing me to Virtual Reality course that sparked my interest in computer vision. I would also like to thank him for supporting me to attend CRC and ISARC conferences which were wonderful experiences. I would like to thank the IIT M Alumni association and the institute for their financial support to attend these conferences.

I would also like to express my sincerest gratitude to my Co-guide, Dr. Ramesh Babu. N for his valuable guidance. His constant encouragements and support have helped me in times of difficulty. Special thanks to him for taking the time out of his busy schedule to guide me. His attention to details feedback on my writing and advice on professional career were very timely and helpful.

We learn not just from the ones who teach us, but also from observing others. I would like to thank the faculty at BTCM for all the lessons taught both inside and outside the classroom. In particular, I would like to thank Dr. Benny Raphael and Dr. Palaniappan Ramu for their valuable feedback on my work and writing. I would also like to thank Dr. Ramamurthy for his timely help for my thesis. I am greatly indebted to Mr. Kavin Kumar and Mr. Mukundan for their advice to join the M.S. program at IIT, which has turned out to be a life-changing experience. They helped me jumpstart a career in construction management. The exposure I gained in working with them and the opportunities they provided for me is incomparable.

This journey would not be half the experience it was without the support of my colleagues and friends in IIT Madras. I would like to thank Anna, Sai, Sanoop, Amritha, Marimuthu, Vijaylakshmi, Yuvraj, Shriram, Velmurugan, Aparna, Srinath and many others whose name I may have forgotten to mention here, but not their help. The late

night discussions, intense arguments and working with many of them in the Autodesk lab has been an enjoyable experience. I would like to thank Abhishek for his valuable support in the technical parts of the research.

Special thanks go to some extraordinary individuals who have been with me, every step of this journey. Sooraj, Nikhil, Ela, Virav, Narsi and Nat have been constant pillars of emotional support. They have been there for the good times and the bad. While a ‘thank you’ seems hopelessly insufficient, it is expressed with utmost gratitude for their precious friendship and support. I would like to thank my friends, Ranjith and Anchal, for the unending conversations - rich, absurd and wonderful, for the spontaneous trips of temporary escapes, the endless devouring of food and for making my stay here a memorable experience. Special thanks go to Ranjith for helping me with the experiments, data acquisitions and technical discussions which were invaluable. I would specially like to acknowledge Ram for the hours we spent brainstorming and the numerous insights from these discussions.

Finally, I would like to thank my parents for all their support and encouragement. All I was, all I am and all I will be, I owe it to them. Amma’s support helped me overcome trying times. My Appa has been a wonderful companion, his enthusiasm, and interest in my work as much as my own. I am thankful for their unconditional love and acceptance. I would also like to thank Hari for introducing me to research life. Last but not least, this thesis is dedicated to both my late grandfathers who would have been proud to see me graduate from IIT M.

With this degree, my M.S journey comes to an end, but not my research journey. I hope to carry with me, all the memories and learnings from the past couple of years. I hope you will enjoy reading this thesis as much as I enjoyed conducting this research.

-Madhumitha

ABSTRACT

Construction progress assessment and monitoring forms an important part of project control. Owing to the inherent complexity of construction activities, traditional progress monitoring techniques are inefficient. There are increasing efforts to automate the data capture system and the progress measurement methods through the adoption of technologies such as BIM. Technological advancements in reality capture devices have made it possible for increasingly automated as-built data collection, which is subsequently integrated with BIM to recognise the progress.

Generation and quality of as-built models influence the subsequent applications such as progress monitoring, quality control, and deviation detection. Laser scanners are widely prevalent, but due to their innate limitations such as mobility issues, the high skill level of personnel for operation, high computational requirements and cost, they have been difficult to adopt for construction environments.

This study aims at investigating alternate commercially available technological devices to capture the reality and generate as-built models. Experimental evaluations were carried out in the laboratory test bed and in a construction site for two different commercially available range imaging devices based on stereo and infrared technologies. The evaluation factors include time efficiency, mobility, ease of scanning, the stability of capture, the accuracy of point cloud models and technological limitations. The generated as-built models are used to assess construction progress through a voxel-based binary classifier algorithm developed for this research. The efficiency of the progress measurement system and the level of the feasibility of using these devices for progress measurement applications are analysed using accuracy, recall, and precision metrics.

It was found that voxel-based binary classifier performed better when compared with other classifiers for as-built models from these range imaging devices. The laboratory test bed results showed the progress classification accuracies exceed 90%. The construction site result showed the progress classification accuracies as 87.54% for ZED camera and 85.62% for Google Tango. It was found that despite both the devices having lower accuracy than conventional technologies such as lasers and photogrammetry, the progress recognition accuracies were comparable to them. It was

found that variations in point densities were one of the-major causes for low accuracy of progress recognition. The results show that despite accuracy limitations, the as-built models generated by both the devices deliver comparable accuracies of progress recognition with respect to other technologies. The most important contribution of this study is the confirmation of feasibility of commercially available range imaging devices for construction progress monitoring application. The results of the experimental evaluations and progress recognition accuracies can be used as a step towards establishing benchmarks for optimum utilization of these devices for other construction applications. Another significant contribution of this work is the development and validation of a prototype of a voxel-based binary classifier that can be used to assess progress quickly.

CONTENTS

ACKNOWLEDGEMENT	iv
ABSTRACT	vi
CONTENTS	viii
LIST OF FIGURES	xi
LIST OF TABLES	xiv
ABBREVIATIONS	xv
NOTATIONS	xvi
1 CHAPTER 1 INTRODUCTION	17
1.1 RESEARCH PROBLEM.....	20
1.2 THESIS ORGANISATION.....	21
2 CHAPTER 2 LITERATURE REVIEW	24
2.1 INTRODUCTION	24
2.2 AUTOMATED AS-BUILT DATA CAPTURE TECHNOLOGIES	25
2.2.1 Earlier technologies	26
2.2.2 Active sensor based technologies	33
2.2.3 Passive sensor-based technologies.....	36
2.2.4 Consumer range imaging devices in construction applications	41
2.3 PERFORMANCE EVALUATION PARAMETERS FOR RANGE IMAGING DEVICES	44
2.4 AUTOMATED PROGRESS RECOGNITION SYSTEM	46
2.4.1 Voxel-based approaches	48
2.4.2 Surface recognition based approaches	50
2.4.3 Other approaches	52
2.5 RESEARCH GAPS	53
2.6 SUMMARY	57
3 CHAPTER 3 OBJECTIVES AND METHODOLOGY	59
3.1 INTRODUCTION	59
3.2 PROBLEM STATEMENT.....	60
3.3 AIM AND OBJECTIVES	60
3.4 SCOPE.....	61
3.5 METHODOLOGY	63
3.5.1 Phase 1: As-built Data Capture Evaluation.....	65

3.5.2	Phase 2: Automated Progress Recognition System Design and Development	66
3.5.3	Phase 3: Progress Recognition System Evaluation	67
3.6	THEORETICAL CONCEPTS	67
3.6.1	Scan-to-BIM registration	67
3.7	SUMMARY	69
4	CHAPTER 4 EXPERIMENTAL SETUP AND EVALUATION METHODS	71
4.1	INTRODUCTION	71
4.2	PHASE 1: AUTOMATED AS-BUILT DATA CAPTURE	71
4.2.1	Hardware Components	71
4.2.2	Software platform for performance evaluation	74
4.2.3	Laboratory test bed	74
4.2.4	Construction site	75
4.2.5	Evaluation parameters	77
4.3	PHASE 2: AUTOMATED PROGRESS RECOGNITION SYSTEM DESIGN AND DEVELOPMENT	82
4.3.1	Design and prototype development	83
4.3.2	Validation metrics	88
4.4	SUMMARY	89
5	CHAPTER 5 RESULTS AND DISCUSSION	91
5.1	INTRODUCTION	91
5.2	PHASE 1: PERFORMANCE EVALUATION IN LABORATORY TESTBED	91
5.2.1	Optimum range of operation	91
5.2.2	Accuracy of as-built models	93
5.2.3	Mobility and time efficiency	95
5.2.4	Influence of lighting conditions	96
5.3	PHASE 1: PERFORMANCE EVALUATION IN CONSTRUCTION SITE	98
5.3.1	Accuracy of as-built models	98
5.3.2	Mobility and time efficiency	99
5.3.3	Influence of lighting conditions	100
5.3.4	Device characteristics	101
5.4	PHASE 3: PROGRESS RECOGNITION SYSTEM EVALUATION	101
5.4.1	Comparison between stereovision and infrared range imaging devices	105
5.4.2	Comparison with other progress recognition methodologies	105
5.4.3	Comparison with other technologies	106
5.5	SUMMARY	107

6	CHAPTER 6 SUMMARY AND CONCLUSION.....	109
6.1	SUMMARY.....	109
6.2	CONCLUSIONS	110
6.3	THEORETICAL CONTRIBUTIONS.....	113
6.3.1	Evaluation of range imaging for construction progress monitoring	113
6.3.2	Comparison between passive and active range imaging devices.....	114
6.4	PRACTICAL CONTRIBUTIONS	114
6.4.1	Development of automated progress recognition system	114
6.5	LIMITATIONS AND FUTURE WORK	115
6.5.1	Extension of current research.....	115
6.5.2	Other areas	116
	REFERENCES.....	117
	APPENDIX.....	123
	CURRICULUM VITAE.....	134
	GENERAL TEST COMMITTEE.....	135

LIST OF FIGURES

Figure 2.1 Component installation status presented in BIM (Ikonen et al. 2013).....	27
Figure 2.2 Application of UWB tags in a construction Site (Cheng et al. 2011)	29
Figure 2.3 Barcode integrated with GIS for construction schedule monitoring and control (Cheng and Chen 2002).....	32
Figure 2.4 Summary of technologies for automated as-built data capture, adapted from (Kopsida et al. 2015).....	55
Figure 3.1 Research Methodology	64
Figure 4.1 Commercially available range imaging devices for capturing reality.....	72
Figure 4.2 ZED Stereovision Camera (Stereolabs, 2016).....	72
Figure 4.3 Project tango development kit	73
Figure 4.4 (a) Configuration 1; (b) Configuration 2;.....	75
Figure 4.5 (a) Construction stage 1 (b) Construction stage 2 (c) Construction stage 3 (d) Construction stage 4.....	76
Figure 4.6 Locations for measuring dimensions for accuracy analysis	78
Figure 4.7 Experimental Setup	81
Figure 4.8 Automated progress recognition workflow	83
Figure 4.9 Pseudo code for labelling voxel occupancy state in as-built model.....	85
Figure 4.10 Pseudo code for labelling voxel occupancy state in BIM	86
Figure 4.11 Pseudo code for comparison of voxel occupancy state in BIM and as-built models	87
Figure 5.1 Influence of object-device distance on resolution of point cloud models generated by ZED Camera.....	91
Figure 5.2 Influence of object-device distance on resolution of point cloud models generated using Tango	92
Figure 5.3 Influence of Object-Device distance on the RMSE of point cloud models generated using ZED camera	92
Figure 5.4 Influence of Object-Device distance on average RMSE of point cloud models generated using Tango.....	93

Figure 5.5 Influence of object-device distance on average dimensional error percentage for point clouds generated by ZED Camera	94
Figure 5.6 Influence of object-device distance on average dimensional error percentage for point clouds generated by Tango	94
Figure 5.7 Comparison of influence of object-camera distance on average scanning time for ZED camera and Tango.....	95
Figure 5.8 Influence of low lighting (7 lux-30 lux) on the average dimensional error for point cloud models generated by ZED Camera	96
Figure 5.9 Influence of low lighting (7 lux-30 lux) on the average dimensional error for point cloud models generated by Tango	96
Figure 5.10 Influence of high lighting (170 lux – 230 lux) on the average dimensional error for point cloud models generated by ZED Camera.....	97
Figure 5.11 Influence of high lighting (170lux-230lux) on the dimensional error for point cloud models generated by Tango	97
Figure 5.12 Comparison of Scanning times for construction site.....	99
Figure 5.13 (a) Original masonry wall with area of interest highlighted in red; (b) Side view of point cloud from ZED: Highlighted area shows multiple surface reconstructed due to rescanning; (c) Front view of point cloud from Tango: Highlighted area shows loss of data due to sunlight interference; (d) Front view of Point cloud from Tango: Highlighted area shows distortion due to rescanning	100
Figure 5.14 (a), (b), (c) Laboratory configurations; (d), (e), (f) Point clouds generated from Tango; (g), (h), (i) Results of progress recognition system: classification legend -green voxels indicate correctly classified voxels, red voxels indicate wrongly classified voxels.....	102
Figure 5.15 (a) BIM of construction stage 3; (b) As-built point cloud model generated by Tango for construction stage 3; (c) Voxel based binary classifier: green voxels indicate “built” voxel & red indicate ‘not-built’	102
Figure 5.16 Accuracy, precision, and recall values for as-built data from ZED camera and Tango (a) Laboratory configuration1 (b) Laboratory configuration 2 (c) Laboratory configuration 3 (d) Construction site	104

Figure 5.17 Performance of classifiers for as-built data from range cameras 105

Figure 5.18 Comparison of confusion matrix metrics for progress recognition using as-built models generated by ZED and Tango against other technologies... 106

LIST OF TABLES

Table 4.1 Comparison of software packages for processing data from zed stereo camera	74
Table 4.2 Stages of construction captured in construction site.....	76
Table 4.3 Experiment details for evaluation of accuracy of as-built models in laboratory test bed	79
Table 4.4 Lighting levels	81
Table 4.5 Voxel occupancy.....	84
Table 4.6 Details of automated recognition system.....	85
Table 4.7 Confusion matrix	88
Table 5.1 Accuracy of as-built model from construction site.....	98
Table 5.2 Voxel colour for progress recognition	103
Table 6.1 Summary of performance evaluation tests.....	111

ABBREVIATIONS

ToF	Time of Flight
GPS	Global Positioning System
RFID	Radio Frequency Identification
LiDAR	Light Radar
LASER	Light Amplification by Stimulated Emission of Radiation
SLAM	Simultaneous Localization and Mapping
RFID	Radio Frequency Identification
SVD	Singular Value Decomposition
BIM	Building Information Models/Modelling
MEP	Mechanical, Electrical, Plumbing
HVAC	Heating, Ventilation, Air Conditioning

NOTATIONS

R	Rotation
s	Scale x
t	Translation
$D_{\text{groundtruth}}$	Dimension measured in BIM
$D_{\text{as-built}}$	Dimension measured in generated point cloud
F_x	Focal length along horizontal direction of image
F_y	Focal length along vertical direction of image
T	Time

CHAPTER 1

INTRODUCTION

Project control relies on availability of efficient and accurate progress assessment for quick decision-making. Owing to the inherent complexity of construction activities, traditional progress monitoring techniques are labour intensive, time-consuming and inefficient (Golparvar-Fard 2011; Navon & Sacks 2007). Further, manual analysis of progress is tedious and subjective, leading to erroneous progress reporting. The time it takes to identify the progress, and detect discrepancies between as-planned and as-built model is proportional to the cost and difficulty in implementing corrective measures (Kopsida et al. 2015). As a result, it becomes imperative that accurate as-built data is

collected with minimal effort and processed automatically to enable efficient project monitoring and control.

The rise of Building Information Modelling to track and visualize construction progress has increased the automation of progress recognition. While numerous commercial software packages such as xBIM, Autodesk BIM 360 help to automate the as-built data collection, they do not address the process of data collection. However, in these methods, the quality of the collected progress data highly depends on the inspector's experience and on the quality of measurements.

In order to automate the process of as-built data collection, various technologies such as Barcodes, RFID, FPS/GIS, strain sensors, lasers, cameras have been used for assessing construction progress. While technologies such as Laser scanners overcome the limitations of RFID, GPS/GIS etc., they have their own limitations. Laser scanners are expensive and require high

computational power for post-processing, high skill level of personnel for operation and lesser mobility. Also, the cost of installation and maintenance of such technologies and the ease of use in construction environments have prevented widespread adoption of this technology.

Range cameras are devices that give a depth value for every captured pixel. There are different techniques and sensors for computing the depth such as Time of Flight sensors and stereo vision technologies, structured light, etc. Recently, range cameras have started to come into the consumer market making them affordable. The reduced costs enable construction personnel to take ownership of these technologies and use them for exploration in applications such as construction progress monitoring . In addition, most of these devices are handheld and require minimal skill levels to operate.

However, their accuracy, range, and operational capabilities have prevented them from being

adopted for construction previously. Due to advancements in hardware and processing software, these technologies can now overcome their prior limitations. However, the extent of feasibility of using these technologies to capture, model and monitor construction progress needs to be evaluated.

This study evaluates two range camera technologies for their feasibility in construction progress monitoring: a passive stereovision-videogrammetry based camera and an active infrared-ToF based camera.

1.1 RESEARCH PROBLEM

The quality of the raw data from any technology needs to be evaluated for its effective utilization prior to its application in other domains. Low-quality raw data would result in higher post-processing time and would require computers with high computation capability. While this data can be improved by better processing techniques, it

would contradict the use of low-cost devices which are time efficient. This study started with the research question “**Can range imaging devices be used for construction progress monitoring application?**”. This question is addressed by exploring the level of accuracy achievable by the as-built models and the progress prediction accuracy using these devices.

1.2 THESIS ORGANISATION

This thesis is organized into six chapters with Introduction forming the first chapter. Each chapter is further divided into the sections. A brief explanation of the contents of these chapters is given below.

- Chapter 2 reviews the literature on technologies used for automated as-built data capture and progress recognition methods. The chapter concludes with research gaps identified from the literature

which serve as the motivation for this work.

- Chapter 3 presents the objectives of this work and its scope. It also discusses the methodology followed to conduct this research along with brief discussions of some theoretical concepts.
- Chapter 4 introduces the range imaging technologies and the testing and evaluation methods for assessing their performance. This chapter also discusses the design and prototype development of an automated progress recognition system along with the metrics for assessing the efficiency of the above system.
- Chapter 5 presents the results of the testing and evaluation of the range imaging devices in the laboratory environment and construction site. It also discusses the performance of the progress recognition

system developed in this research and the implications of the results from a construction perspective.

- Chapter 6 summarizes the contributions of this work with the important conclusions. Further, it presents the potential areas for future research.

CHAPTER 2

LITERATURE REVIEW

2.1 INTRODUCTION

The previous chapter gave an outline on the need for automated as-built data collection for efficient construction progress monitoring. In order to answer the research question, a literature study was conducted. The review consists of three sections. In the first section, the technologies for automated as-built data capture for construction progress monitoring applications are identified and reviewed. In the second section, a review of the parameters for evaluating the performance of different technologies are discussed. In the last section, different approaches for automated progress recognition are reviewed.

2.2 AUTOMATED AS-BUILT DATA CAPTURE TECHNOLOGIES

This section discusses various automated data collection technologies used in construction and presents it in three sections. The first section briefly examines certain major works in earlier technologies for capturing construction as-built data and progress monitoring. These include barcodes, RFID, GPS/GIS and UWB. In the next section, prior research in the area of active sensors such as laser scanners is analysed, followed by a critical review of work done on passive sensor-based technologies such as photogrammetry, videogrammetry etc. The final section reviews research works on the application of commercially available range imaging devices and the challenges associated with their application in construction field.

2.2.1 Earlier technologies

2.2.1.1 Barcode

Barcodes are used in construction monitoring by evaluation and management of prefabricated components and then tracing it back to the planned schedule of dispatch and then backtracking to the construction progress (Cheng and Chen 2002). Usually, the data collected from barcodes are implemented in three phases of a construction project: Design, Manufacturing, and Construction.

They are commonly used to track materials and infer the construction progress from them. However, limitations such as low storage capacity, durability, readability etc. have limited their widespread adoption in construction (Kopsida et al. 2015; Vähä et al. 2013).

2.2.1.2 Radio Frequency Identification (RFID)

RFID tags have been explored commonly for prefabricated construction for applications such as material and labour tracking for inventory management, productivity measurements, progress measurements (Valero et al. 2015; Ikonen et al. 2013; Xie et al. 2010). The information management for RFID tags require large data storage capabilities. In particular, for

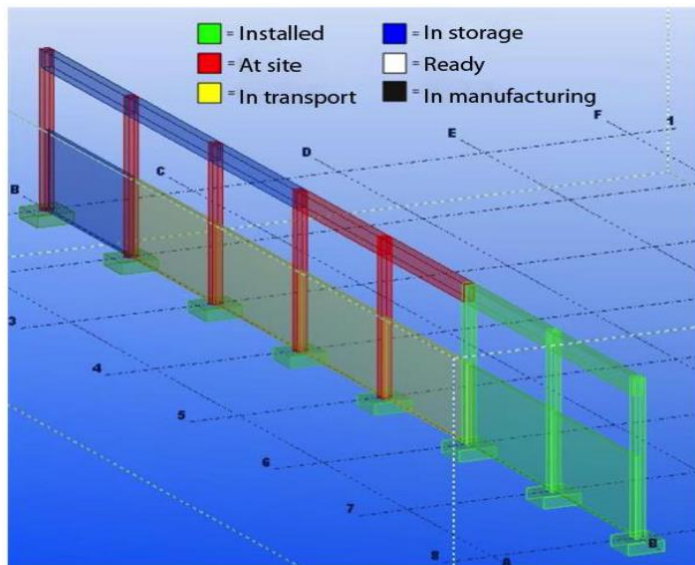


Figure 2.1 Component installation status presented in BIM (Ikonen et al. 2013)

elements which are not present in the line of sight, tracking with such tags becomes difficult. Ikonen et al. presented pilot studies in using RFID for tracking logistics and their status (shown in Figure 2.1) in a construction site (Ikonen et al. 2013).

RFID has also been integrated with other technologies for effective construction monitoring. For example, Wang et al. developed a method for using RFID to track different components and visualizing construction progress by integrating the information with BIM (Wang et al. 2013). However, not all construction elements can be tagged with RFIDs. Further, the technology requires additional investments on equipment installations and human effort are required for capturing the data. For cast-in-situ construction, the tags cannot be used to measure quantity. Construction activities requiring rework cannot be measured using this technology as it cannot capture the geometric information of the as-built component.

2.2.1.3 Ultra-wide band

Similar to RFID tag, Ultra-wide band (UWB) provides real-time location tracking to resources that are equipped with UWB tags. It works on short pulse RF waveform based on time domain principles of electromagnetic theory. It has a



Figure 2.2 Application of UWB tags in a construction Site (Cheng et al. 2011)

higher range, measurement accuracy, and immunity to interference when compared with RFID (Cheng et al. 2010).

Cheng et al. also evaluated the performance of UWB for construction resource tracking in a construction site (Cheng et al. 2011). Although the ultra-wide band is accurate than RFID, it has inherent disadvantages such as the requirement for modeling, association of tags with the equipment etc. In addition, the range of UWB is limited and semantic information about the construction elements cannot be captured.

2.2.1.4 Global Positioning System (GPS) and Geographical Information System (GIS)

Global Positioning System (GPS) and Geographical Information System (GIS) have been used for automatic data collection to monitor real-time construction progress (Burbano et al. 2016). Real-time information of materials and equipment can be tracked using GPS and GIS systems. This helps in obtaining the real-time vehicle locations, navigation assistance, and drive speed heading information. All these data could be integrated with real-time information

management system to track the progress of construction (Pradhananga and Teizer 2013; Li et al. 2005). Cheng and Chen developed a method for integrating GIS with barcode for construction material tracking, schedule monitoring, and control (Cheng and Chen 2002). Figure 2.3 shows the operational structure of the schedule

monitoring and control system developed by the study.

However, the technology can be used only when

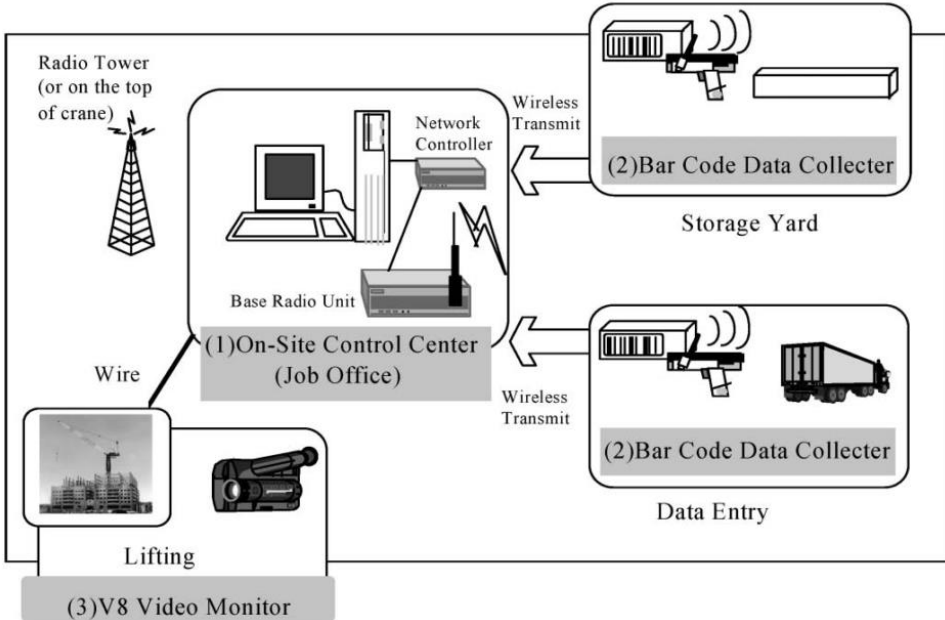


Figure 2.3 Barcode integrated with GIS for construction schedule monitoring and control (Cheng and Chen 2002)

the activities have a direct relation to the distinct materials used. In addition, GPS is inefficient in areas where the signal reception is low and cannot be used indoors. Semantic information about the

construction component cannot be captured by GIS, thus limiting its potential usage for construction monitoring.

2.2.2 Active sensor based technologies

Active sensors utilize emitted light for capturing reality. The emitted light can be laser or infrared. There are different mechanisms used to sense the depth using emitted light such as Time-of-Flight (ToF), structured light etc. In ToF, the time taken for the emitted light to strike an object's surface and reflect back is recorded. Based on this information and intrinsic parameters of the sensors used, the 3D coordinate of the point is calculated. Structured light projects a pattern of light on an object and the distortion of the pattern is analyzed to determine the depth of objects in the scene. Laser scanning has many benefits such as high accuracy, dense point clouds that provide geometric and semantic information (when integrated with an RGB camera), large operational range, etc. 3D laser scanning is based on ToF or

structured light techniques for computation of depth of a scene. In ToF technique, the time elapsed in the detected of the reflected light is used to compute the depth of the scene. This process results in a collection of points, which can be combined to form accurate 3D models.

High-end laser scanners can acquire 3D with accuracy in the range of 3mm at 50m with a resolution of 12mm at 100m (Bosché 2010). Due to their accuracy, they are often used for quality control (Akinci et al. 2006), obstacle tracking and interference detection (Gordon & Akinci 2005), and monitoring (Sacks et al. 2003). However, high precision cannot be achieved at object edges and spatial discontinuities (Brilakis et al. 2011). Turkan et al. could obtain significant positive results for progress monitoring using 3D laser scanner with a simple 3D model (Turkan et al. 2010). Zhang and Arditi were able to develop an automated progress recording system that did not require any human intervention at the site or for

processing the point clouds (Zhang and Arditi 2013).

While many of these studies report a high accuracy of progress recognition, factors such as computational effort of generating them and the skill level required from the user were not addressed. Additionally, laser scanners are expensive and require considerable time for capturing large areas through multiple scans. In addition, they generate dense 3D point clouds, which imposes high cost and time for computation and processing. For obtaining a full 3D reconstruction of a building, several control points have to be set up in order to stitch different laser scans together, increasing the data acquisition time (Hajian and Becerik-Gerber 2010; Sacks et al. 2003). The discontinuity in spatial data, the need for regular sensor calibrations and a slow warm-up time are also of the other disadvantages of this technology (Golparvar Fard et al. 2012). From a construction perspective, the as-built state

needs to be captured frequently (daily/weekly/biweekly/monthly). As a result, technologies which are cost effective and are able to capture and generate point clouds in real-time are preferred.

2.2.3 Passive sensor-based technologies

Passive sensors utilize illumination to capture reality. They rely on natural and artificial illumination to detect the RGB information of the scene and compute the depth through algorithms. Both photogrammetry and videogrammetry are based on passive sensors. It requires more user intervention to generate the 3D scene when compared to laser scanning (Sternberg et al. 2004), but lower equipment cost and faster data acquisition time make it more viable for construction applications. The actual state of the construction site is detected by photogrammetric surveys and is then used for automated comparison with the planned state for early

detection of deviations in the construction process (Braun et al. 2015).

The level of accuracy of the point cloud generated from these technologies depends on the camera's resolution and the bundle adjustment algorithm (Triggs et al. 2000). The accuracy of point clouds generated using photogrammetry has been assessed by many research works (Bosche et al. 2009; Triggs et al. 2000). Common methods of accuracy assessment include resolution of point cloud generated, dimensional errors and deviation of point cloud model with respect to ground truth model (Bhatla et al. 2012; El-Omari and Moselhi 2011).

With the advancements in Structure-from-Motion (SfM) techniques for the 3D reconstruction, photogrammetry has been increasingly used to track construction progress (Sirmacek and Lindenbergh 2014; Bhatla et al. 2012; Brilakis et al. 2011). Initially, images captured were registered using manual and semi-automatic

methods for 3D reconstruction, and these images were used for comparison with BIM to identify components constructed (Golparvar-Fard et al. 2009a). Time-lapsed, image-based recognition upon comparison with BIM component for progress identification has also been experimented (Golparvar-Fard et al. 2009b; Ibrahim et al. 2009; Zhang et al. 2009). In these works, the changes in the time lapsed images are searched and recognized, and finally compared to a 3D model to determine the progress. However, the recognition is non-invariant; lighting conditions and occlusions limit the efficiency of the system. While these can be overcome through prior planning during data capture, it requires considerable preparatory efforts by the user. This further increases implementation problems in practice. Further, some parts of the data capture and 3D reconstruction are not automated completely (Kopsida et al. 2015; Golparvar-Fard et al. 2011b; Zhu and Brilakis 2009). User intervention is required for giving prior

information on the sequence of photographs and the images need to be captured such that there is sufficient overlap between them for a successful reconstruction.

Videogrammetry is based on the same principle as photogrammetry, except the relationship between the images in each frame will be known a-priori since each frame is sequentially recorded in a video. Due to higher overlap between subsequent frames, videogrammetry based 3D reconstruction can generate a better as-built model with a higher degree of automation (Brilakis et al. 2011; Fathi and Brilakis 2011; Tissainayagam and Suter 2005). Schops et al. reported an error of 5% in depth map measurement using existing automated reconstruction methods (Schöps et al. 2016). Brilakis et al. presented a videogrammetry framework to acquire dense 3D point clouds using stereo cameras which are accurate, automatic and cost-efficient (Brilakis et al. 2011). Changes in illumination levels, abrupt, and fast movement of

the camera and noise can interfere with feature extraction. These can cause failure in matching of features between successive frames (Remondino, Fabio; El-Hakim 2006). The automation of videogrammetry is not always successful in practical applications and the spatial data retrieved from videogrammetry is at the expense of their measurement accuracy (Zhu and Brilakis 2009).

It was observed that the majority of literature focussed on 3D reconstruction methods from imaging and videogrammetry of construction sites. While the data processing has become easier, these techniques require a high computational cost with frequent human intervention, making them less attractive for repetitive progress monitoring activities. Commercially available range imaging devices offer inbuilt 3D reconstruction SDK suites which facilitate real-time as-built model creation. This fully automated 3D reconstruction reduces the processing requirements from the end-user's side.

2.2.4 Consumer range imaging devices in construction applications

Passive sensor based range imaging has been investigated in many construction applications such as progress monitoring, and ergonomics monitoring, quality conformance, safety checks, visualizations etc. (Ishida 2016; Kim and Caldas 2013; Naticchia et al. 2013; Weerasinghe et al. 2012). Chae and Kano developed a method for estimating the 3-D data through application in an actual construction site with locational information in the 3D space of time series from images using SfM technique (Chae and Kano 2007). Brilakis et al. presented a videogrammetry stereo camera for acquiring spatial data of infrastructure and progressively reconstructed a scene from the images (Brilakis et al. 2011). Compared with photogrammetry, the entire reconstruction process using videogrammetry needs little human intervention, since the search of 2D locations of a target point in different images

can be accomplished by measuring or tracking interesting features between consecutive video frames (Serby et al. 2004). Hence, videogrammetry has been adopted as an appropriate measurement technique for applications like automatic industrial product inspections (Graves and Burner 2001). Accuracy and resolution analysis of point clouds generated by Kinect sensors were studied (Zennaro et al. 2015; Rafibakhsh et al. 2012). Shell-shell deviation analysis have also been employed to evaluate the accuracy of point clouds generated by photogrammetry (Majid et al. 2009).

Active sensor based range imaging technologies using structured light, ToF and thermal imaging have also been used in areas of worker management and activity detection in construction. The Kinect sensor has been experimented in construction applications. It is a consumer-grade range camera uses triangulation and multiple pseudo-random pattern light ray

projection measured with an integrated RGB camera to capture reality. Data from Kinect sensors have been used for worker activity classification using Gaussian mixture based classifiers (Kim and Caldas 2013). Experimental evaluation of 1st and 2nd generation sensors for operational range, point cloud resolution and depth accuracy were also studied (Zennaro et al. 2015).

Low-quality raw data would result in higher post-processing time and would require computers with high computation capability. However, the details about the process of reconstruction from most consumer range devices remains a black box. Hence, the quality of as-built point cloud models can be evaluated through experimental evaluations. Further, it is necessary to test these technologies in laboratory conditions and in the construction site to understand its performance.

2.3 PERFORMANCE EVALUATION PARAMETERS FOR RANGE IMAGING DEVICES

With improvements in hardware and software capabilities, commercially available range images have increased capabilities than their predecessors. However, the feasibility of using these reality capture devices depends on the type of application it is being used for. The parameters which influence the performance of the reality capture devices can be categorized into two areas:

- Parameters from construction perspective: quality of as-built models, time efficiency, mobility, ease of use, level of automation, the minimum and maximum range of usage etc.
- Parameters from computer vision perspective: sensor resolution, orientation/angle of sensor with reference to the object, influence of

object characteristics on sensor, the accuracy of as-built models, resolution of as-built models, the influence of ambient illumination, Field of View, noise, calibration etc.

The above performance evaluation parameters were chosen by analyzing prior research works on construction application. Researchers have explored the methods for evaluating the accuracy of the as-built models in terms of geometry and point distribution density of the point cloud (Froehlich and Azhar 2016; Zennaro et al. 2015; Golparvar-Fard et al. 2011c). Kopsida et al. noted that factors, such as range of operation, mobility and time required for preparation, capturing, processing, play a decisive role in the adoption of technology for construction applications (Kopsida et al. 2015). Further, ambient lighting conditions and stability of devices during constant use also influence their adoption (Froehlich and Azhar

2016; Pătrăucean et al. 2015). From literature, it is clear that the following parameters are found to be critical from a construction perspective.

- Optimum range of operation
- Accuracy of as-built models
- Mobility and time efficiency
- Influence of lighting conditions
- Device characteristics

Though these parameters are not exhaustive, they provide critical insights into the performance of range imaging devices.

2.4 AUTOMATED PROGRESS RECOGNITION SYSTEM

After generating the as-built models, they need to be brought to the same coordinate system as the BIM. This is achieved by aligning the as-built model with the BIM using control points. The alignment can be achieved by manually selecting the control points, or semi-automated where the user assists the system or fully automated where there is no user interference (Golparvar Fard et al.

2012; Bosche and Haas 2008). The theoretical concept is explained in section 3.6.

After successful alignment of the as-built model with the BIM, both the models will be in the same coordinate system and superimposed on each other. The progress recognition is split into two steps. In the first step, the progress is detected by verifying the existence an element/object in the same location in both the models. Then, the detected progress is measured cumulatively. In order to validate the detection of progress, confusion matrix metrics such as accuracy, recall and precision are used. These metrics are widely used in object recognition and classification in computer vision.

Several types of recognition methods such voxels, surface, point to point which use classifiers such as binary, linear SVM, point-to-point, probabilistic etc. have been explored by past works to detect construction progress. These approaches are reviewed in this section.

2.4.1 Voxel-based approaches

A voxel is a cuboid in 3D space, which is usually an array of discretized grid-like elements. They are similar to pixels in a bitmap. They consist of regularly spaced vertices defined in the global coordinate system. The progress of a construction site can be measured by segmenting the scene into discrete voxel cells and by marking them as free or occupied, independent from the data collection technique since only the position is required. For construction progress recognition, each cell which intersects a triangle of the BIM/containing adequate number of points, can then be labelled as BIM occupied. Later, all voxels, which are labelled as occupied, can be labelled 'as-built' if the number of points from the as-built point cloud model is also inside the cell is above a predefined threshold; otherwise, they are marked as not built.

Simple voxel threshold based binary classifiers were first explored by Bosche and Haas for automated object retrieval using point thresholds

and plane deviation of as-built point cloud from laser scanning (Bosche and Haas 2008). The occupancy state of a voxel (empty or occupied) depends on the accuracy of scanning technology. In another method called ray casting, all voxel cells in the field of view of a scanning position are assigned the state visible if the ray from the scanning position passes the centre of the voxel without intersecting a surface triangle; and labelled unknown otherwise (Bosché et al 2010). Based on certain heuristics, this voxel-based approach can be extended to handle occlusions (Braun et al. 2016; Sirmacek and Lindenbergh 2014). Tuttas et al. developed a probabilistic approach based on voxel comparison using photogrammetric point clouds and BIM (Tuttas et al. 2014).

Bayesian probabilistic model, which learned the dynamic thresholds for classification, was implemented using linear Support Vector Machine (SVM) classifier for recognizing

progress deviations (Golparvar-Fard et al. 2015). An advantage of the voxel based method is that it allows a higher tolerance for point clouds with larger dimensional errors and plane deviations. However, it should be noted that in the above most of the above studies, as-built point clouds from laser scanners were used as input for the classifiers. These point clouds are dense and have uniform point density. As a result, machine learning based classifiers might not be able to achieve similar progress recognition accuracies for sparse and non-uniform point clouds.

2.4.2 Surface recognition based approaches

Surface based approaches use triangles in the 3D representation of a BIM to measure the surface covered by as-built points for progress detection. The matching parameters can include the point-to-surface distance, point surface colour as well as normals. If an as-planned point cloud has been used for alignment and if it has been constructed, the Euclidean distance between each point pair is

sufficient. If a point is recognized as belonging to a surface, the surface covered by this point has to be calculated. To decide whether the recognized points are sufficient to confirm the existence of the building element, the number of recognized points and the mean distance between them is compared with the same parameters of a point set sampled uniformly on the triangle surface. If the deviations are above a certain threshold, the recognized points are not dense enough or close together to represent a continuous surface.

Tuttas et. al proposed an approach that matched the relevant points from the as-built point cloud model directly onto the triangulated surfaces of the as-planned model (Braun et al. 2015). Some research approaches used a surface based recognition metric for progress recognition; these approaches recognize an object when the recognized surface exceeds a minimum threshold (Nicolas et al. 2012; Bosche et al. 2008). It should be noted that the surface-based approach is more

difficult for point clouds which have a lower uniform density. Additionally, the method requires a lower root mean square deviation of the point cloud plane.

However, as noted previously, point clouds from passive photogrammetry and range imaging contain considerable dimensional errors are often obtained commonly from passive range imaging cameras. Thus, these methods might not be feasible for the current study.

2.4.3 Other approaches

Zhang & Arditi developed a method that counts the number of points in the related portions of the point clouds generated by photogrammetry and compared it against point cloud generated by laser scanners (Zhang and Arditi 2013). Rebolj et al. compared a segmented site image and a model using an algorithm that recognizes the differences between element features (Rebolj et al. 2008).

2.5 RESEARCH GAPS

The earlier technologies discussed in this section have inherent limitations such as the lack of mobility, high cost, requirement of highly skilled personnel for operation and absence of semantic information. While laser-based as-built data acquisition systems are highly accurate, factors like the high equipment cost, mobility issues, large post processing times, limit its widespread adoption in construction sites. Even though photogrammetry addresses most of the above concerns, a large part of 2D to 3D reconstruction is not completely automated. A summary of all the technologies for construction monitoring is shown in Figure 2.4. Black cells indicate good performance, while the grey and white cells indicate mediocre and poor performance respectively (Kopsida et al. 2015).

It can be seen that, while lasers are accurate, they perform poorly in many other parameters. Only static imaging, videogrammetry and commercial

range imaging devices have the maximum parameters compliance under mediocre and good performance. However, as noted previously, the former two technologies involve considerable user interference and are at present computationally expensive.

Consumer range imaging devices have become

Comparison parameter ↓ Technology →	Barcode	RFID	GPS/GIS	UWB	Laser Scanners	Static Imaging	Video-grammetry	Commercial range imaging devices
Time Efficiency	instant information retrieval	instant information retrieval	Time taken for retrieval	instant information retrieval	Time needed for scans + post processing time	Manual information assignment and registration	Time taken for 3D reconstruction	Time needed for scans
Cost	Cost of scanning device	cost of installation & maintenance	Cost of Device	installation & maintenance cost	Expensive	Consumer Hardware	Consumer hardware	Consumer hardware
Range	Limited	Limited	High	Limited	High	Average-High	Average-High	Limited-Average
Accuracy	Geometric information not captured.	Geometric information not captured	Geometric information not captured	Geometric information not captured	Geometric information captured. Very accurate	Geometric information captured. Less accuracy	Geometric information captured. Accurate	Geometric information captured. Accurate
Level of Automation	Automated capture, no data analysis	Automated capture, no data analysis	Automated capture, no data analysis	Automated capture, no data analysis	Fully automated	partially automated data acquisition, automated data analysis	Partial automation, automated data analysis	Fully automated data acquisition & data analysis
Required Preparation	Installation and maintenance of tags	Installation and maintenance of tags	Minimal setup required	Installation and maintenance of tags	set the equipment (<1hour)	Minimal setup required	Minimal setup required	Minimal setup required
Skilled personnel training	None	none	None	None	trained personnel for scanner operations	Trained personnel for post processing	Trained personnel for post processing	None
Mobility	Handheld equipment	Handheld equipment	Handheld equipment	Handheld equipment	large & heavy equipment	Handheld equipment	Handheld equipment	Handheld equipment

Figure 2.4 Summary of technologies for automated as-built data capture, adapted from (Kopsida et al. 2015)

affordable and evolved to enable automated 3D reconstruction. Thus they are seen as alternatives for automated as-built data capture. However, research on the application of these technologies for progress monitoring has not been studied due to their limited accuracy and range. Further, the performance of these technologies and their associated benchmarks have not been explored in detail in laboratory controlled conditions and in construction site.

Additionally, modification of the existing progress recognition methods are required to suit the as-built point clouds from range imaging device. Most of the progress recognition methods use as-built data from laser scanners. These as-built point clouds have high accuracy and a dense point cloud resolution. Hence, the threshold parameters used by these research works cannot be directly adopted for progress recognition using as-built data from range imaging devices. It was also noted that the computational time and effort required for

these approaches were not recorded in any of the research works. These constitute a knowledge gap which this work aims to address. Such a study can help to evaluate the accuracy of the generated as-built models, operational conditions influencing the quality of as-built point cloud models and the level of progress prediction accuracy achievable using these data.

2.6 SUMMARY

This section discussed the research works for earlier technologies such as Barcodes, RFID, UWB, GPS/GIS, their advantages and limitations. Prior research works which explored the use active and passive sensors for construction was also discussed. Further, research on the application of range imaging devices for construction such as worker productivity, progress monitoring etc. were reviewed.

Additionally, the evaluation parameters to assess the performance of range imaging technologies

were reviewed. The section concluded with the review of progress recognition methods such as voxel based, surface recognition based approaches and the corresponding classifiers used.

CHAPTER 3

OBJECTIVES AND METHODOLOGY

3.1 INTRODUCTION

The previous chapters discussed in detail on the need for automated monitoring in construction and the necessity of using range imaging devices for reality capture. The chapter concluded with the identification of knowledge gaps in literature for using these devices for construction progress monitoring. This chapter builds on the previous chapters and defines the broad definition of the problem statement, the aim and objectives of this work, its scope, and the methodologies followed.

3.2 PROBLEM STATEMENT

The need to quickly assess the progress of building construction and the challenges involved in using consumer range imaging technologies for automated as-built data capture and progress recognition was discussed in the previous chapters. Owing to mobility, high cost, skill level, ease of use, range imaging technologies can effectively aid in capturing construction progress. However, the quality of the generated as-built models from these technologies needs to be evaluated. This study focuses on the evaluation of two consumer range imaging devices for their feasibility for construction progress monitoring application.

3.3 AIM AND OBJECTIVES

The aim of this study is to evaluate the capability of two range imaging devices based on stereovision and infrared technologies for capturing as-built data and assess its level of feasibility for monitoring construction progress.

This is achieved through three objectives, which are as follows

- To study the performance of two range imaging devices: passive stereovision and active infrared range imaging devices in the Laboratory Test bed and the Construction Site.
- To design an Automated Progress Recognition System and develop a prototype
- To evaluate the performance of the Automated Progress Recognition System based on conventional object recognition metrics.

3.4 SCOPE

The performance evaluation parameters of the devices for this study are limited to evaluating the optimum range of operation, accuracy of as-built

models, mobility & time efficiency, the influence of lighting conditions, device characteristics including scan speed and stability. This study focusses on the capturing as-built information for Masonry and Concreting components only.

3.5 METHODOLOGY

The methodology followed in this study is shown

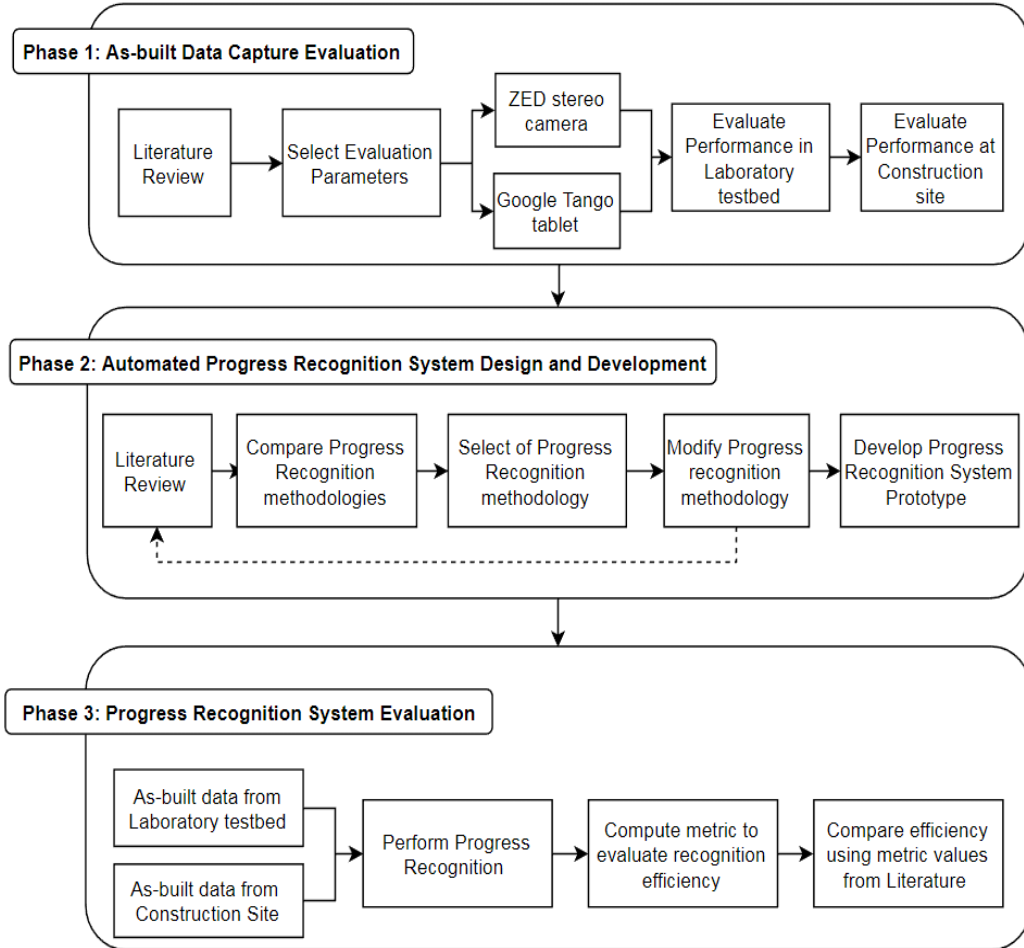


Figure 3.1 Research Methodology

in Figure 3.1.

3.5.1 Phase 1: As-built Data Capture Evaluation

In Phase 1 of the research methodology, the existing literature is reviewed to understand the gaps in using other technologies for automated construction progress monitoring and application of range imaging based cameras in construction environments. These were elaborated in section 2.2. Then, the evaluation parameters for testing the performance of the devices are selected from the literature based on its relevance in construction applications and was discussed in section 2.3. Finally, the performances of the two range imaging cameras are evaluated for the selected parameters in the laboratory test bed and the construction site.

3.5.2 Phase 2: Automated Progress Recognition System Design and Development

In Phase 2, an Automated Progress Recognition System was designed based on comparison and modification of existing methodologies. A prototype of the system was developed for testing the as-built data.

This phase involves a review of the literature to understand and compare existing progress recognition methods and was discussed in section 2.4. Based on the review, the selected method is modified to suit the scan data. Then the modified method is evaluated for its performance by conducting tests using as-built data from laboratory test bed and construction site. A prototype of the progress recognition system is developed for this purpose.

3.5.3 Phase 3: Progress Recognition System Evaluation

In Phase 3, the efficiency of Automated Progress Recognition System prototype and the as-built data from both the devices were evaluated using object recognition metrics such as accuracy, Recall, and Precision. For this phase, the as-built data from both laboratory test bed and construction site is evaluated. The performance of the progress prediction of the system and the as-built data was compared with the values reported in the literature.

3.6 THEORETICAL CONCEPTS

3.6.1 Scan-to-BIM registration

The scan-to-BIM registration process is in Phase 2, under the design and development of the automated progress recognition system. The as-built point cloud model obtained from the device need to be registered to the same coordinate as the BIM. To achieve this, the procedure described by

Horn was used to coarsely align both the models and achieve sufficient overlap (Horn 1987). Horn's method finds the optimal transformation between two point sets M (model) and D (data) based on n pairs of corresponding points. A transformation in the 3D coordinate system comprises of 7 degrees of freedom: a translation t , a rotation R and a scale s in x , y , z directions. Since one corresponding pair of points provides three equations (one in each dimension), $n=3$ results in nine constraints which are enough to calculate the seven unknown transformations. The point sets from the as-built model and the BIM containing the three corresponding pairs are mostly detected manually and make the only manual part of the registration process (Bosché 2010). Cloud Compare, a software platform designed for manipulating point clouds was used in this research. It's 'Point based alignment tool' aligns two models based on three user-defined control points (Daniel GM, 2015). After the coarse registration, the alignment is refined by using

Iterative Closest Point algorithm (ICP). A maximum root mean square error of 2cm is used to stop the ICP registration.

3.7 SUMMARY

This chapter discussed the objectives of the research work and its scope. The research methodology followed in this work was also described. The methodology was divided into three stages. Phase 1 involves literature review of earlier technologies, application of range imaging devices in construction and progress recognition methods. The research gap identification, selection of evaluation parameters for range imaging devices were also discussed in this subsection. Phase 2 involved design and development of a prototype of an automated progress recognition system. The third phase of the research is the evaluation of the progress recognition system for as-built point cloud models from laboratory test bed and construction site. In

addition, this chapter also discussed the theoretical concepts the scan-to-BIM registration process.

CHAPTER 4

EXPERIMENTAL SETUP AND EVALUATION METHODS

4.1 INTRODUCTION

In the previous chapter, the research methodology and the broad phases of the research were discussed. This chapter focuses on parts of phase 1: automated as-built data capture evaluation and phase 2: automated progress recognition system design and development. Section 4.2 introduces the range imaging devices along with the software used for evaluation. Further, the section also discusses the laboratory test bed, the construction site and the experiments for the parameters selected for this research. Section 4.3 elaborates the details of the design and development of the automated progress monitoring system of Phase 2. This section also discusses the metrics used for assessing the efficiency of the progress recognition system.

4.2 PHASE 1: AUTOMATED AS-BUILT DATA CAPTURE

In this section, the hardware and software that were used to capture reality and the experimental methodologies for performance evaluation of these devices and the quality of the as-built models generated are discussed.

4.2.1 Hardware Components

Currently, there are numerous commercially available range imaging devices for capturing reality. A brief comparison of the technical specifications and the cost is shown in Figure 4.1.

Based on the sensor resolution, specified range, Field of View (FoV) and cost of the currently available range imaging devices, ZED camera and Google Tango (previously known as Project Development Kit) were selected for evaluation in this study. These devices are employed as test cases for evaluation of the underlying technology. However, for ease of understanding, they are referred by their brand names wherever applicable.

Specification ↓ Devices →	Kinect	Structure Sensor	Project Tango Development Kit	ZED Camera	Duo Stereo camera	Bumblebee stereo camera
Active sensors	IR camera with 640x480 pixels at 30 Hz	VGA IR camera 640 x 480	4 MP 2 μ m RGB-IR pixel sensor	-	-	-
Passive sensors	RGB camera with 640x480 pixels at 30 FPS	QVGA 320 x 240 at 30/60 FPS	Fish eye RGB camera	4 MP 2 μ m RGB camera	750x 480 to 320 to 120	1.3MP at 3.8mm RGB
Depth sensing method	Time of Flight	Structured light	Time of flight	Visual SLAM	NA	NA
Specified Range	0.5m to 4.5m	0.4m to 3.5m+	0.4m to 4m	0.5m to 20m	0.23m to 2.5m	0.5m to 4.5m
FOV	Horizontal: 57 Vertical: 43	Horizontal: 58 Vertical: 45	Horizontal: 68 Vertical: 38	Horizontal: 93 Vertical: 61	Horizontal: 170 Vertical: NA	Horizontal: 66 Vertical: NA
Additional sensors	IMU	-	IMU	-	IMU	-
Precision	-	0.5mm at 40cm; 30mm at 3m	-	-	0.1 to 0.3mm within specified range	-
Supporting Platform	Xbox 360 Xbox one Windows	iOS	Linux, Windows	Android, Linux, Windows	Linux, OSX, Windows	Windows
Cost	\$100	\$379	\$445	\$445	\$599 ~ \$1200	~ \$3500

Figure 4.1 Commercially available range imaging devices for capturing reality

4.2.1.1 ZED stereovision camera

ZED camera (representative image shown in Figure 4.2) is a stereoscopic passive RGB camera that uses stereo camera lens sensors and algorithms to reconstruct the 3D scenes from the stereo images. The camera has a maximum resolution of 2208x1242 pixels resolution at 15FPS. It comes with software SDKs that can be used to calibrate and create 3D reconstructed models. The ZED SDK processes the disparity map on the host



Figure 4.2 ZED Stereovision Camera (Stereolabs, 2016)

machine requiring NVidia GPU with CUDA API6 or greater. The camera was designed mainly for autonomous navigation and mapping (Burbano et al. 2016).

The camera's maximum depth perception range is 20m. The ZED explorer is the primary software that can be used to record a video in '.svo' file format (Stereolab's format) which is then processed by the ZED Fusion package to create disparity maps from the stereo images and subsequently create a 3D point cloud. Each frame from the video is converted into a point cloud and registered successively using visual odometry, enabling the creation of a point cloud represented in 3D space. While the same process can be done in real-time using ZED Fusion, the algorithm does not work efficiently and has the possibility of crashing or resulting in a distorted point cloud. However, this glitch may be resolved in future SDK futures.

4.2.1.2 Project Tango development kit

Project Tango Development Kit is an Android development level tablet (shown in Figure 4.3) that uses Infrared technology coupled with an RGB camera to capture depth. The tablet consists of a motion tracking RGB camera, Accelerometer, light sensor, Infrared projector, Barometer, Compass, GPS, Gyroscope. The infrared-based tablet uses Time-of-Flight (ToF) to detect the depth of the object being scanned. It incorporates Simultaneous Localization and Mapping (SLAM) for mapping its location to create a point cloud representation of the scanned object in 3D space.



Figure 4.3 Project tango development kit (Google, 2015)

R-TAB Map was used for the creation of point cloud. It directly generates the 3D point cloud and the meshed surfaces, which are available for upload and export in '.obj' file

format for further processing. The device self-calibrates when the app starts, after which the user can use it for capturing scenes.

4.2.2 Software platform for performance evaluation

There are many commercially available software platforms, which processes 2D images/videos to output as an as-built model using 3D reconstruction techniques. The choice of software is influenced by the skill level of the user, level of automation, quality of the generated as-built point cloud model and time taken for reconstruction. In order to determine the best software for 3D reconstruction for the ZED stereo camera device, some commonly available software was tested. A set of 80 photographs were given as input for all software. The time taken for reconstruction was recorded. The accuracy of reconstruction was measured by analysing the number of points reconstructed and the area of the reconstructed surface. Finally, the percentage error in reconstruction is calculated by comparing the area reconstructed to the actual area of the object scanned. The results of these two tests are tabulated in Table.

Table 4.1 Comparison of software packages for processing data from zed stereo camera

Software Package	Time Taken (s)	No. of Points Reconstructed	Reconstructed Surface Area (mm²)	Error in Reconstruction (%)
Remake	103	21,185	952	3.05
Context Capture	117	16,722	430	56.21
VisualSFM	4548	12,086	370	62.32
ZED Fusion SDK	430	2,09,361	966	1.63

It can be seen that ZED Fusion SDK has the least error in 3D reconstruction and least processing time. Hence, ZED Fusion was chosen for reconstructing 3D as-built point cloud models. For Tango, at the time of evaluation, only the R-TAB Map was available for capturing reality. Hence, it was selected for capturing as-built data for Tango.

4.2.3 Laboratory test bed

Tang et al. stressed the need for research on evaluation of the performance of as-built modelling methods using test beds that simulate the entire range of factors affecting on-site construction performance (Tang et al. 2010). Laboratory and on-site evaluation of device performance help to establish standardization in test sets and performance measures contributing to benchmarking. In this context, comparison of the scanning

device in ideal conditions (simulated by laboratory experiments) and on-site conditions can help understand the capabilities and limitations of these devices in construction applications.

A test bed setup was designed in the laboratory to study the performance of the devices under varying conditions such as lighting and object-camera distance. The model configurations in the test bed are shown in Figure 4.4. The test bed background was designed as a white background to bring the object into sharper focus. The objects of interest were centered in the test bed and captured with no occlusions. Both the devices were handheld during their usage.

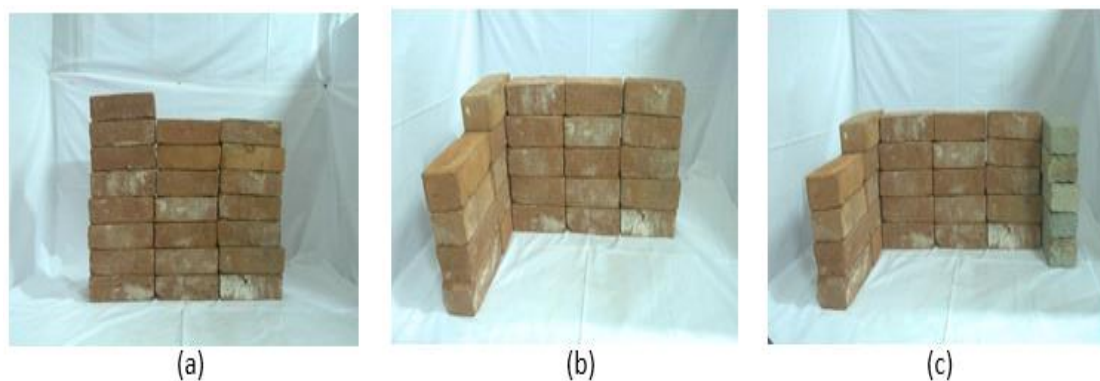


**Figure 4.4 (a) Configuration 1; (b) Configuration 2;
(c) Configuration 3**

Two lighting conditions ‘Low’ and ‘High’ were simulated with corresponding varying lux ranges using an external lamp. The minimum distance of the camera from the object was 0.5m and the initial level of the camera was at the ground level of the object. The model configurations were designed such that they imitate a typical room with masonry walls in a construction site. Configuration 1 consists of one plane, while configurations 2 & 3 have increasing planes with increasing complexity.

4.2.4 Construction site

The devices were tested for capturing four different stages of construction. The elements captured include masonry walls, concrete floors, columns, beams, and finished walls, tiled floors, windows, and doors.

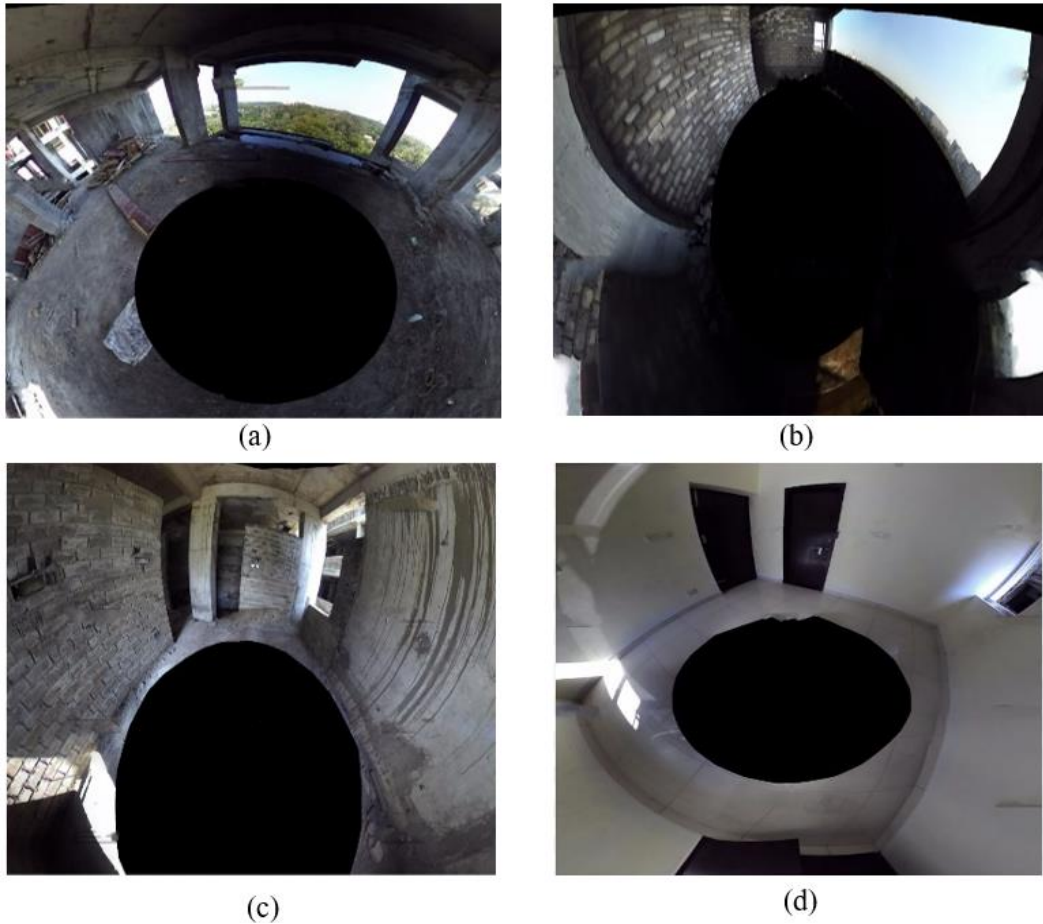


Figure 4.5 (a) Construction stage 1 (b) Construction stage 2 (c) Construction stage 3 (d) Construction stage 4

A 360° panoramic view of each stage is shown in Figure 4.5. Table 4.2 shows the details of the stages of construction and the components captured. Stage No.3 and Stage No.4 are similar to each other while the areas captured in other stages are unique.

Table 4.2 Stages of construction captured in construction site

Stage No.	Stage Description	Components Completed
1	Frame	Columns, beams, floor, ceiling
2	Frame + Partial Masonry	Columns, beams, floor, ceiling, partial masonry
3	Frame + Full Masonry	Columns, beams, floor, full ceiling, masonry
4	Completed Room	Fully constructed room including plaster, paint, tile finishing, windows, doors, electrical switchboards

4.2.5 Evaluation parameters

The evaluation parameters were arrived at by review of literature of different technologies as explained in section 2.3. The performance evaluation parameters tested for this research are listed below.

- Optimum range of operation
- Accuracy of as-built models
- Mobility and time efficiency
- Influence of lighting conditions
- Device characteristics

The parameters were tested for both the laboratory test bed and the construction site with a few exceptions. Since the models used for testing in the laboratory test bed were small, the device characteristics could not be fully evaluated. For the construction site, the optimum range of operation experiment was not performed since it was not feasible to capture the whole room in one scene while simultaneously varying the object-device distance. Furthermore, the experiments for studying the influence of lighting conditions were simulated only in the laboratory test bed. However, the effect of lighting was visually observed at the construction site.

To determine the variation of point clouds between different datasets, four datasets were collected and analysed for the optimum range of operation, accuracy of as-built models and influence of lighting conditions experiments. Each dataset is a unique set of as-built models which were captured under same experimental conditions. The variation in values between the datasets is represented through error bars with standard deviation of 1. Each dataset contains point clouds generated at object-device distance increments of 0.1m. Thus, the total sample size was 60 point cloud models and 64 for Tango. For these experiments, the variation in values are represented by an error bar showing both the positive and negative standard deviation.

4.2.5.1 *Optimum range of operation*

Two experiments were performed for determining the optimum range of these technological devices. In the first experiment, the influence of distance of the object from the device on the resolution of point cloud generated is studied. The object-device distance is increased sequentially by 0.1m and the object is captured at every increase

in the distance. The 3D reconstruction process used by these range imaging devices is a black box; each pixel of the captured image does not translate to the point cloud. Consequently, the point density in the point cloud does not correspond to the number of pixels in the 3D image. Hence, the resolution of the point cloud needs to be determined after the 3D reconstruction to assess the density. For each point cloud generated at different distances from the devices, the resolution of the point cloud is calculated. The resolution is the number of points present in 1cm^2 of the point cloud.

In the second experiment, the influence of distance of the object on the distortion of the object plane is studied. The scans at different distances are aligned and superimposed on a ground truth model. The distance between the point cloud and the ground truth model planes are measured in Cloud Compare software and represented as Root Mean Square Error (RMSE). The distance range with maximum average resolution and the minimum average RMSE is determined as the optimum range for operating the devices. Within this range, the optimum capability of the devices can be exploited since the accuracy is the highest.

4.2.5.2 Accuracy of as-built models

For evaluation of the dimensional accuracy of the as-built point cloud model, dimensions from the as-built model are compared to the actual dimensions. The deviation is expressed as a percentage ratio of the deviation with respect to the actual dimensions (Bhatla et al. 2012; Golparvar-Fard et al. 2011c). In this study, the term

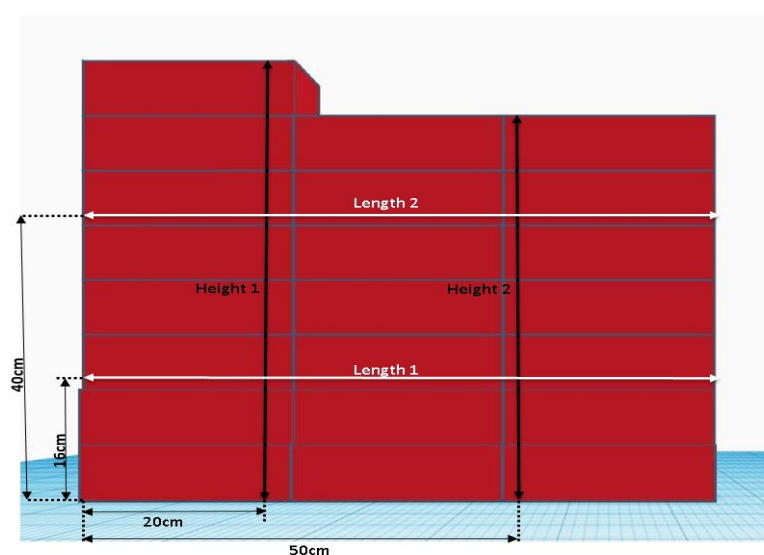


Figure 4.6 Locations for measuring dimensions for accuracy analysis

‘dimensional error’ is used to denote the error in the measured lengths for an object. For the laboratory test bed, 16 as-built point clouds of the three configurations under varying simulated lighting conditions, and object-device distance were captured and analyzed. In each of the point cloud, four measurements were recorded for analysing the dimensional error. Thus, the total sample size for the experiment was 64 measurements for each device. The locations of these measurements in the model are shown in Figure 4.6

For the construction site, the dimensional accuracy was analyzed for the as-built data from the four stages of construction and compared against actual dimensions. The percentage dimensional error is calculated using equation 4.1.

$$\text{Average dimensional error (\%)} = \frac{\sum_{i=1}^n \frac{D_{ground\ truth} - D_{as-built}}{D_{ground\ truth}}}{n} \cdot 100 \quad (4.1)$$

The actual dimensions of elements captured in both the laboratory test bed and the construction site are measured using Leica Disto off-the-shelf laser surveying device with a range of 0.05 to 150m and an accuracy of 1mm. In the as-built point cloud model, the corresponding dimensions are manually extracted. The deviation between these two values is given an input to Equation 4.1. Meshlab interface was used to extract the as-built point cloud dimensions. Details of this experiment is given in Table 4.3

Table 4.3 Experiment details for evaluation of accuracy of as-built models in laboratory test bed

Dataset	
No. of as-built models for ZED	15 models (captured at 0.1m increments for the range 0.7m to 2.1m)
No. of as-built models for Tango	16 models (captured at 0.1m increments for the range 0.6m to 2.1m)
No. of dimensions measured in each model	4
Software for measuring As-built model dimensions	MeshLab

4.2.5.3 Mobility and time efficiency

A determining factor in the adoption of a technology for construction is its ease of use and the time efficiency. Often multiple scans are required to capture one single floor in a construction site. Hence, lightweight devices that can withstand long durations of usage are preferred. The mobility of the devices was determined by the level of effort required by the user during data capture.

The total time consumed by each device from the start of scanning until the generation of point cloud was recorded for as-built data in the laboratory test bed and the construction site (equation 4.2).

$$Total\ time = T_{device\ preparation} + T_{scanning} + T_{post\ processing} \quad (4.2)$$

The influence of Field of View (FOV) on scanning time is also examined. The FOV is calculated using equation 4.3 and equation 4.4.

$$FOV\ Vertical = 2 \cdot \arctan\left(\frac{0.5 \cdot height}{F_y}\right) \quad (4.3)$$

$$FOV\ Horizontal = 2 \cdot \arctan\left(\frac{0.5 \cdot width}{F_x}\right) \quad (4.4)$$

where F_x and F_y are Focal lengths, and width and height denote the image dimension on the sensor.

4.2.5.4 Influence of lighting conditions

Stereo cameras are light dependent for 3D reconstruction, as the algorithms require well-illuminated scenes for finding correct stereo matches between the images. Infrared-based sensors are sensitive to external light interference. To test the influence of lighting conditions, a Low light and High light was simulated in Laboratory to imitate lighting conditions in the Construction site. The experimental setup is shown in Figure 4.7.

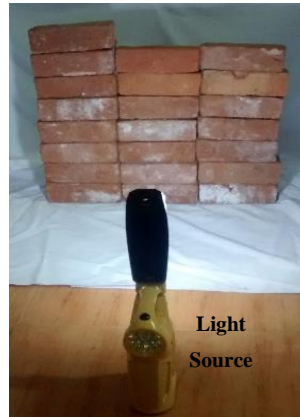


Figure 4.7
Experimental Setup

The as-built models generated under the two lighting conditions were studied for the variation in dimensional errors using the method described in section 4.2.5.2. The sample size was 60 measurements for ZED camera with a split up of 15 observations with 4 measurements analysed for dimensional error in each observation. For Tango, the sample size was 64 measurements with a split up of 16 observations with 4 measurements analysed for dimensional error in each observation. The final dimensional error under each lighting condition was represented as the average error of the four measurements in each observation.

Table 4.4 Lighting levels

Lighting Levels	Observed Range in Construction site (Lux)	Simulated Range in Laboratory Test bed (Lux)
Low	10-20	7-30
High	180-220	170-230

For the construction site, the lighting conditions cannot be controlled. Hence, distortions in the as-built point cloud models were assessed qualitatively.

This experiment focuses only studying the influence of the intensity of light under two extremities (low and high light). Additional factors such as light spectrum, object characteristics and orientation of the device were not studied.

4.2.5.5 Device characteristics

A clockwise scanning path was adopted for both the devices. The maximum angular velocity with which both devices can capture without any localization loss was determined by trial and error method. Device stability was evaluated by considering the ease of use, maximum power capacity and stability of devices in construction environments.

4.3 PHASE 2: AUTOMATED PROGRESS RECOGNITION SYSTEM DESIGN AND DEVELOPMENT

This section discusses the design and prototype development of the automated progress recognition system. Further, the validation metrics for assessing the performance of the as-built data for progress recognition applications are also elaborated.

4.3.1 Design and prototype development

Automated progress recognition methodologies such as surface-based recognition, point-to-point comparison, Support Vector Machines, and probabilistic binary

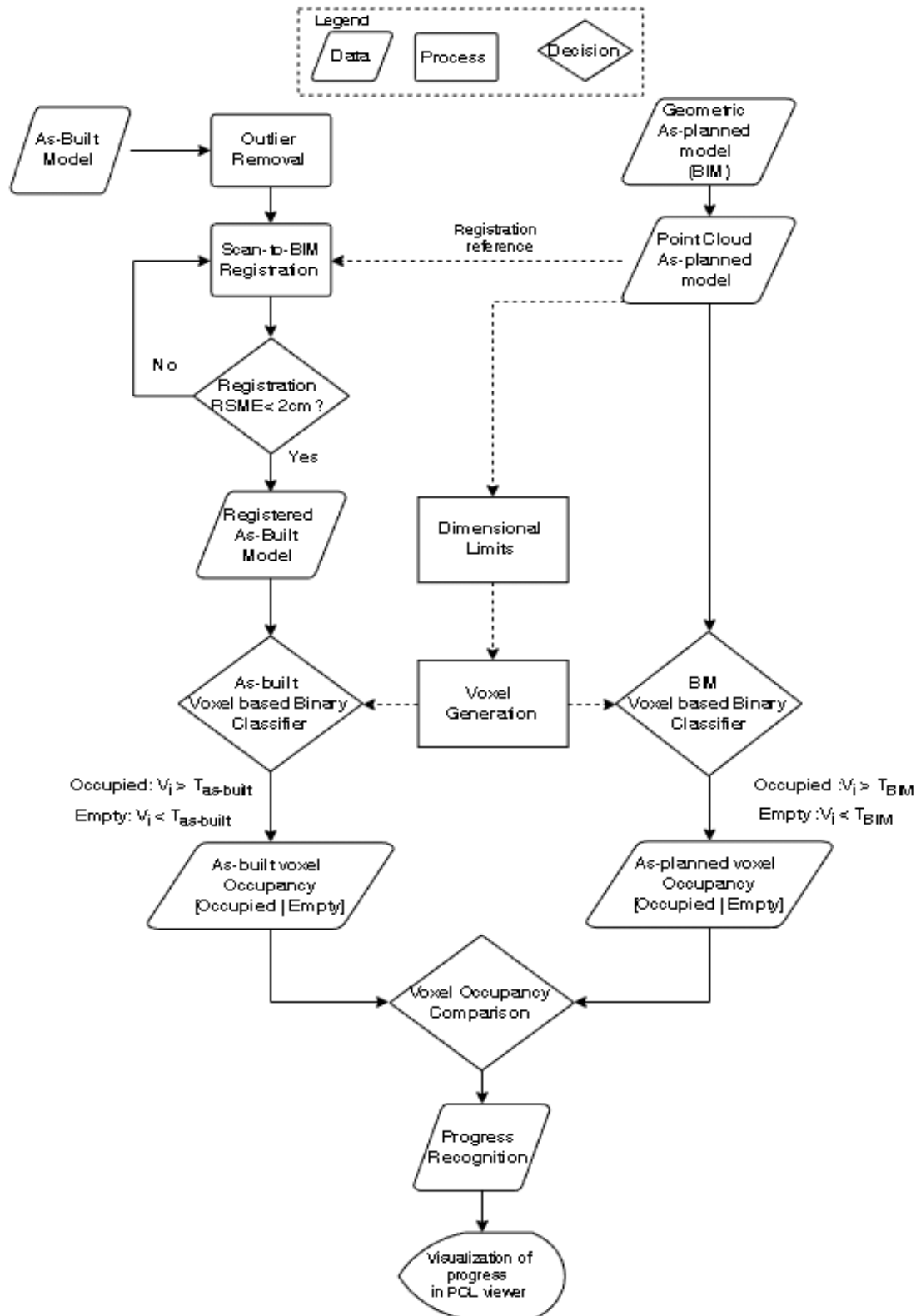


Figure 4.8 Automated progress recognition workflow

classification have been explored in prior research works (Braun et al. 2015; Golparvar Fard et al. 2012; Brilakis et al. 2011). In these works, the as-built models were generated by lasers scanners and photogrammetry, which differ from the as-built models from range imaging devices in terms of accuracy, point cloud density etc. Thus, the progress recognition method needs to be modified. The classification method developed by Boschè et al. involving comparison of point-to-point BIM and as-built models was altered for this research work (Bosche and Haas 2008). The algorithm workflow is shown in Figure 4.8 uses a basic binary voxel-to-voxel classifier for progress recognition.

In the first step in Figure 4.8, the as-built model from the devices is refined by removing outliers. The number of neighbors to analyse for each point is set to 50, and the standard deviation multiplier is set to 1. All points which have a distance larger than 1 standard deviation of the mean distance to the query point will be marked as outliers and removed. The output from this process is a filtered point cloud. Simultaneously, the geometric BIM is converted into a point cloud representation (Point cloud As- planned model).

In the next step, the point cloud as-planned model is used as a reference for registering the as-built model to the same coordinate system. The registration is performed using Horn’s method and refined by Iterative Closest Point (ICP) algorithm through Cloud Compare software interface. The registration is accepted if the RMSE is less than 2cm. After successful registration, the dimensional limits of the as-planned model is extracted for voxel generation. Based on these limits, the 3D space is discretized into a finite number of voxels along the three Euclidean axes (x, y, and z). The voxels generated in this step are used as a backdrop for comparison of voxel occupancy in both the as-planned and as-built models in the subsequent steps.

Table 4.5 Voxel occupancy

	Occupied	Empty
As-built model (A)	$V_i > T_{as-built}$	$V_i < T_{as-built}$
BIM (B)	$V_i > T_{BIM}$	$V_i < T_{BIM}$
Binary Classifier labelling	TRUE	FALSE

Then, the voxel based binary classifier is employed for the as-planned model and the as-built model. This classifier categorizes the occupancy state as either ‘Occupied’ or ‘Empty’ for each of the discretized voxel using threshold values (Table 4.5). In the penultimate step, the voxel occupancy for the as-built model and the as-planned model

Table 4.6 Details of automated recognition system

Input	<i>BIM (.obj' file format)</i>
	<i>As-built point cloud model (.obj' file format)</i>
Output	<i>Confusion Matrix values (TP, TN, FP, FN)</i>
Voxel Size	<i>11cm x 11cm x 11cm</i>
ZED: 'Built' Classification Threshold ($T_{as-built}$)	<i>40</i>
Tango: 'Built' Classification Threshold ($T_{as-built}$)	<i>250</i>
BIM: 'Built' Classification Threshold (T_{BIM})	<i>13</i>
Prototype Development	<i>C++ integrated with Point Cloud Library (PCL)</i>

Algorithm 1: Voxel Occupancy Labeling for as-built point cloud model

```

Input:    A [as-built point cloud model]
          Vijk [voxel grid]
          Tas-built [threshold for ZED and Tango]
Output:   {Aijk} As-built Voxel Occupancy
1   Start with A, V
2   for all Vi,j,k do
3       Aijk=0
4       for all points in A do
5           if [point within Vijk]
6               | Store point in Aijk_count
7           end if
8       end for
9       if A_count>Tas-built
10          | Aijk is occupied
11      else
12          | Aijk is empty
13      end if
14  end for

```

Figure 4.9 Pseudo code for labelling voxel occupancy state in as-built model

is compared to detect the progress. If the corresponding voxel in each model is occupied, the voxel is classified as ‘built’.

The details of the parameters used in the progress recognition system are shown in Table 4.6. Based on the point cloud resolution values determined earlier, the classification threshold values were extrapolated for the voxel size by considering the lowest resolution in the optimum operating range.

The binary classifier is used to detect if the number of points in each voxel points exceeds the threshold points for the input models. If the threshold is satisfied, the voxel is classified as ‘occupied’; if not, it is classified as ‘empty’ (refer Figure 4.8). The voxel edge length was fixed at 11cm through trial and error method to detect both smaller built components and larger components.

Algorithm 2: Voxel Occupancy Labeling for as-planned BIM point cloud model

Input: B [as-planned BIM point cloud model]
 V_{ijk} [voxel grid]
 T_{BIM} [threshold for BIM]

Output: $\{B_{ijk}\}$ As-planned Voxel Occupancy

```

1     Start with B, V
2     for for all  $V_{i,j,k}$  do
3          $B_{ijk}=0$ 
4         for all points in B do
5             if [point within  $V_{ijk}$ ]
6                 Store point in  $B_{ijk\_count}$ 
7             end if
8         end for
9         if  $B_{ijk\_count}>T_{BIM}$ 
10              $B_{ijk}$  is occupied
11         else
12              $B_{ijk}$  is empty
13         end if
14     end for

```

Figure 4.10 Pseudo code for labelling voxel occupancy state in BIM

The three configurations from the laboratory test bed and Stage 3 as-built model from the construction site generated using ZED camera and Tango were used for evaluating the Progress Recognition System. Eight as-built models were evaluated. It should be noted that the BIM as-planned model is taken as the ground truth model to determine the accuracy of progress prediction.

The workflow shown in Figure 4.8 outputs a viewer displaying the recognized progress along with confusion matrix values: Accuracy, Recall, and Precision. The pseudo codes of the algorithms for voxel occupancy labelling for as-planned BIM and as-built point cloud models are shown in Figure 4.9 and Figure 4.10.

The progress recognized in the penultimate step in the workflow consists of ‘built’ voxels; the ones that are classified as ‘occupied’ in both the models (True Positives) while the voxels classified as ‘empty’ in the as-built model are the ones that are classified as ‘False Negative’. If the voxels are classified as ‘empty’ in both the models, then these voxels are denoted as ‘True Negatives’; while voxels classified as ‘empty’ in the as-planned model are denoted as ‘False Positive’. The pseudo code for this occupancy states of each voxel is shown in Figure 4.11. In this study, only the prediction accuracy of the ‘built’ voxels are considered for performance evaluation.

Algorithm 3: Voxel Occupancy Comparison

```

Input:   {Aijk} As-built Voxel Occupancy
         {Bijk} As-planned Voxel Occupancy
Output:  Confusion Matrix [TP,TN,FP,FN]
         Cstate [Construction State]
1   Start with Aijk, Bijk
2   for all i do
4     if Aijk=Bijk
5       TP++
6       Cstate=Built
7     else if Aijk is occupied and Bijk is empty
8       FP++
9     else if Aijk is empty and Bijk is occupied
10      FN++
11    else
12      TN++
13    end if
14  end for

```

Figure 4.11 Pseudo code for comparison of voxel occupancy state in BIM and as-built models

For the purpose of monitoring, the voxels recognized as “built” needs to be converted to an IFC format. The volume occupied by the voxels is labeled as a part of the

corresponding BIM elements using methods like semantic labeling (Han et al. 2015; Golparvar Fard et al. 2012; Li et al. 2008). The current research is limited to the comparison of as-planned (BIM) and as-built models only for progress recognition.

4.3.2 Validation metrics

The three configurations from the laboratory test bed and Stage 3 as-built model from the construction site by both ZED camera and Tango tablet were used for evaluating the Progress Recognition System. Eight as-built models were evaluated. The data from both the devices were analysed using the progress recognition system methodology as mentioned section 4.4. A confusion matrix was used to analyse the performance of the system by using the metrics: Accuracy, Recall, and Precision. Confusion matrix/error matrix helps in visualization of the performance of an algorithm (Stehman 1997). Accuracy is the ratio of correctly predicted cases to the total dataset (equation 4.5). Recall is the proportion of actually positive ratio cases that were also predicted positive (equation 4.6). It is an indicator of the completeness of the recognition. Precision is the proportion of predicted positives vales which are also actually positive (equation 4.7). It is an indicator of the correctness of detection. The desirable values for each of these metrics differ based on the type of algorithm and its purpose. Hence there is no consensus on the optimum range for these metrics (Powers 2011).

Table 4.7 Confusion matrix

		BIM	
		<i>Actual Positive</i>	<i>Actual Negative</i>
As-built Data	<i>Predicted Positive</i>	True Positive(TP)	False Positive (FP)
	<i>Predicted Negative</i>	False Negative (FN)	True Negative (TN)

$$Accuracy = \frac{\sum True Positives + \sum True Negatives}{\sum Total \ number \ of \ Voxels} \quad (4.5)$$

$$Recall = \frac{\sum True Positives}{\sum True Positives + \sum False Negatives} \quad (4.6)$$

$$Precision = \frac{\sum True\ Positives}{\sum True\ Positives + \sum False\ Positives} \quad (4.7)$$

From a construction point of view, it is desirable to have a good compromise between the precision and recall values so that the progress prediction can be trusted with a higher confidence (Dimitrov and Golparvar-Fard 2014; Hui, L. and Brilakis 2013; Bosché 2010). Finally, the values of Accuracy, Recall, and Precision of this system are compared with the values found in literature for other progress recognition systems/classifiers to assess the system's performance.

4.4 SUMMARY

This section described the experimental setup, range imaging devices and evaluation methods for phase 1 of the research methodology: automated as-built data capture. Section 5.2 elaborated on the technological devices used for this research, its hardware specifications and the software platforms used for evaluation. Additionally, the objects used for capture in the laboratory testbed and the construction site were discussed. The details of the experimental methods for assessing the five evaluation parameters were discussed in this subsection. In section 4.3, the design and development of an automated progress recognition system for the as-built data generated by both the range imaging devices were elaborated. The metrics for evaluating the efficiency of progress recognition were also discussed.

CHAPTER 5

RESULTS AND DISCUSSION

5.1 INTRODUCTION

In this chapter, the results of the As-built Data Capture Evaluations from Phase 1 is discussed. Further, the results of the Progress Recognition System Evaluation from Phase 3 is also discussed. The results of evaluations in Phase 1 are segregated into two sections: Laboratory test bed and Construction site. Under each subsection, the discussions also include the implication of the results for construction environments.

5.2 PHASE 1: PERFORMANCE EVALUATION IN LABORATORY TESTBED

5.2.1 Optimum range of operation

The variation of resolution of the as-built model with respect to the distance of object for ZED camera and Tango tablet is shown in Figure 5.1 and Figure 5.2. It was observed that ZED camera did not detect the scene when the object-device distance was within 0.6m. The resolution of as-built point cloud model generated by ZED camera decreased beyond 1.1m distance of the device from the object. The resolution of the point cloud depends on the sensor pixel resolution and the stereo correspondences. For ZED camera, the Back Illumination (BI) CMOS sensor resolution is 2 micron pixels. With an increase in object-device distance, the ZED camera's resolution limits the capture of

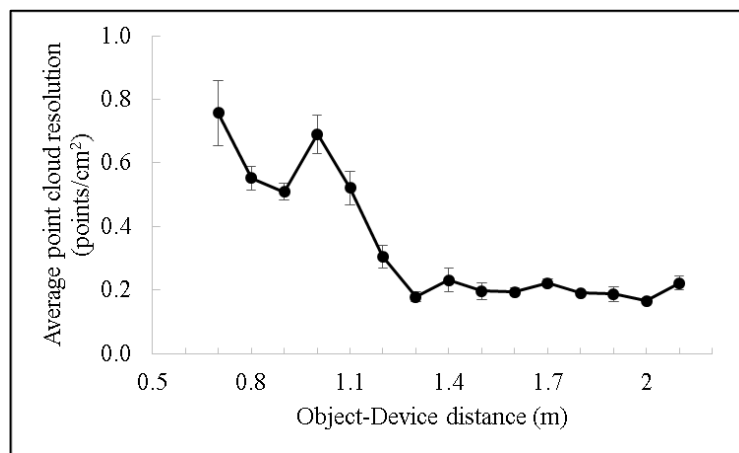


Figure 5.1 Influence of object-device distance on resolution of point cloud models generated by ZED Camera

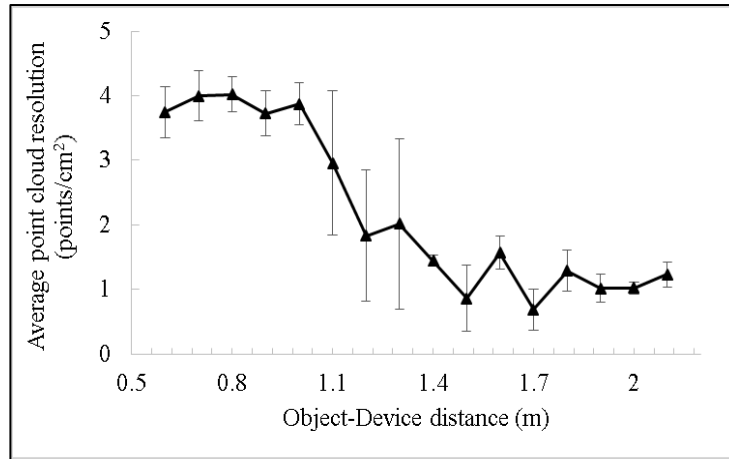


Figure 5.2 Influence of object-device distance on resolution of point cloud models generated using Tango

unique features which in turn affects the 3D reconstruction. Thus with an increase in distance, the sensor’s resolution causes a decrease in the resolution of the point cloud. From the error bars in Figure 5.1 and Figure 5.2, it was observed that ZED camera had a lower standard deviation of the average point cloud resolution compared to Tango. For Tango, the resolution decreased after 1.1m distance mark. The RGB IR camera in Tango has a resolution of 2 μ m. Similar to the behaviour observed in ZED Camera, with an increase in distance, Tango’s sensor resolution causes a decrease in the number of points per unit area.

In the second experiment, the variation in RMSE of the point cloud models with an increase in distance of the object from the camera is studied. Figure 5.3 and Figure 5.4 show the RMSE for ZED and Tango respectively. The resolution of the point cloud depends on the sensor pixel resolution and the stereo correspondences. ZED camera

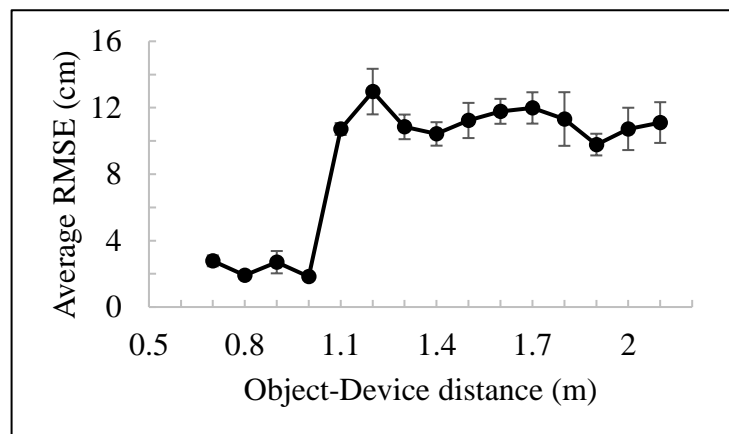


Figure 5.3 Influence of Object-Device distance on the RMSE of point cloud models generated using ZED camera

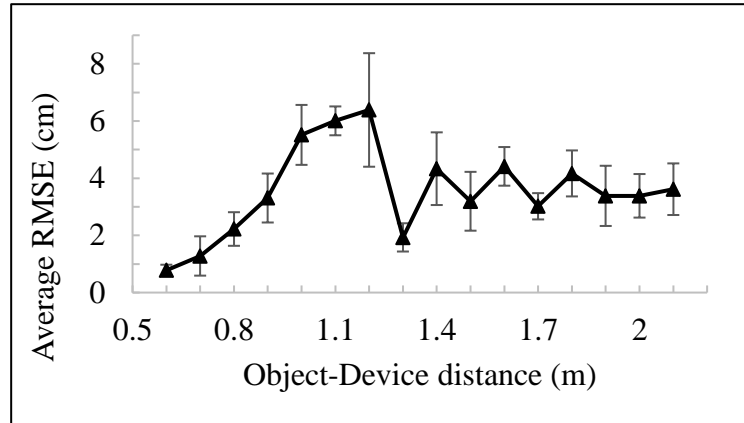


Figure 5.4 Influence of Object-Device distance on average RMSE of point cloud models generated using Tango

was observed to have a lower error in the range 0.7m-1m while Tango tablet had lower RMS error in the range 0.6-1.1m. The RMSE depends on both the sensor resolution and the 3D reconstruction algorithm. For ZED, with an increase in distance, the object of interest becomes smaller, thus fewer correspondence points are reconstructed.

However, for Tango, the range of RMSE is significantly lower than that of ZED. This is due to its ToF technique of data capture, which provides more dimensionally accurate 3D reconstruction.

For both the devices, the sensor resolution influences the resolution of the point cloud generated. Higher resolution of point clouds helps capture the scene more accurately. For Tango, the variation of the resolution and the RMSE with an increase in object-device distance was observed to be unpredictable beyond 1.1m. However, the reason for this behaviour could not be determined from the current dataset. Additionally, it was observed that the standard deviation of the four samples at each object-device distance showed minimal variation within 0.6m to 1m for Tango, was increasing drastically beyond that limit.

From the above experiments, the optimum range of usage (with maximum resolution and minimal RMSE) for ZED was 0.7-1m while for Tango it was 0.6-1.1m.

5.2.2 Accuracy of as-built models

After determination of the optimum range of operation in the above section, the dimensional error in the point clouds generated within the optimum range is calculated.

The dimensional error in the point clouds generated by models in the laboratory test bed was analyzed using the method described in section 4.2.5.2.

Figure 5.5 and Figure 5.6 show the variation of dimensional accuracy with reference to the object-device distance for ZED camera and Tango respectively. From Figure 5.5, ZED camera has an average dimensional error of 1.40% in the optimum distance range of 0.7m -1m while Tango has a dimensional error of 1.20% in the optimum distance range of 0.6m-1.1m (Figure 5.6).

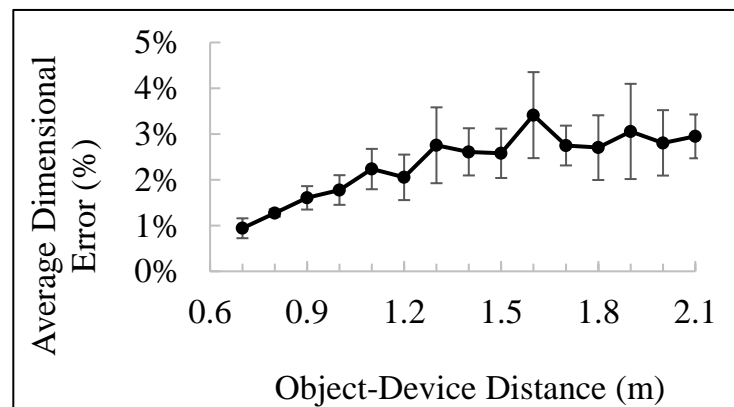


Figure 5.5 Influence of object-device distance on average dimensional error percentage for point clouds generated by ZED Camera

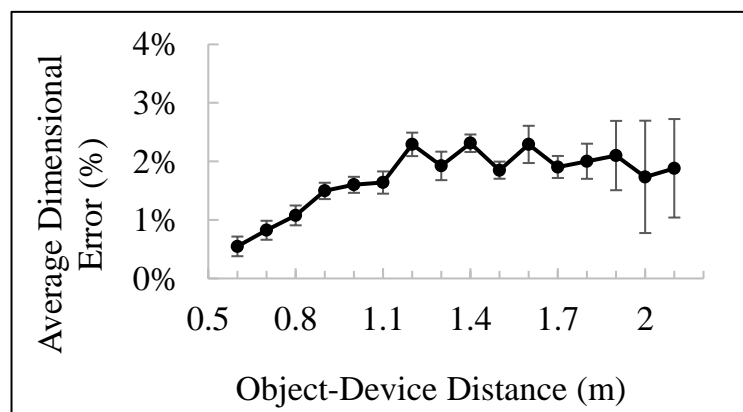


Figure 5.6 Influence of object-device distance on average dimensional error percentage for point clouds generated by Tango

The error bar for the dimensional error from the 4 datasets were plotted with the standard of the four datasets. From the error bar in of the above figures, it was observed that within the optimum range, the variation of the average dimensional error for the 4 datasets was minimal for both the devices. However, this variation increased with the increase in the object-device distance.

For ZED, the average resolution is 0.6 points/cm² for point cloud models generated in the range of 0.7m-1m (Figure 5.1). For Tango, the average resolution is observed as 3.7 points/cm² in the range of 0.6m-1.1m (Figure 5.2).

The dimensional accuracy of Tango tablet is higher than ZED camera due to the technique of Range imaging as elaborated in the previous evaluation. However, the resolution of the point cloud generated by both the devices is sparse. Lower resolution affects the accurate capture of smaller objects. Thus, in construction environments, components such as reinforcements, electrical fixtures were not captured accurately.

5.2.3 Mobility and time efficiency

The models captured in the laboratory test bed are smaller, compared to the elements in a construction site. As a result, the scanning time is much shorter and the post-processing time is negligible. The variation of time required for scanning with respect to the distance of the object from the device is shown in Figure 5.7. It can be observed from the figure that the scanning time is inversely proportional to the distance of the object from the device. In particular, beyond 1.1m, the scanning time stabilizes for both the devices. This is due to the Field of View (FOV) of the devices which is calculated as described in section 4.2.5.3.

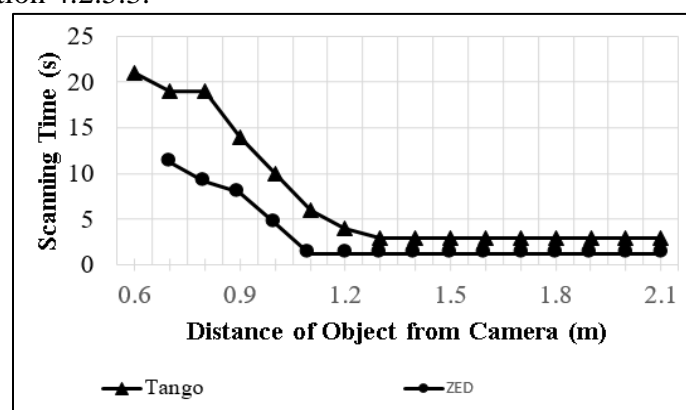


Figure 5.7 Comparison of influence of object-camera distance on average scanning time for ZED camera and Tango

Using equation 4.3 and equation 4.4, the horizontal and vertical FOV of ZED camera were determined as 93° and 61° respectively. Similarly, Tango tablet was determined to have a horizontal FOV of 68° and a vertical FOV of 38°. During the evaluation of the optimum range of operation experiment, it was observed that at 0.6 to 0.8m object distance, the device’s FOV limits the scanning area visible to the camera, resulting in longer scanning time. However, with an increase in object-camera distance, the FOV

increases and as a result, the scanning time decreases. It was observed that due to larger FOV, ZED camera was able to scan areas much faster than the Tango tablet. While the laboratory test bed evaluations show the influence of FOV on capture speed, further implications of FOV- scanning time in a construction site is discussed in section 5.3.2.

5.2.4 Influence of lighting conditions

All three configurations were captured and as-built point cloud models were generated in two lighting conditions as described in section 4.2.5.4. The average dimensional error for the 4 sets of point cloud data at each object-device distance in low light condition is shown in Figure 5.8 and Figure 5.9.

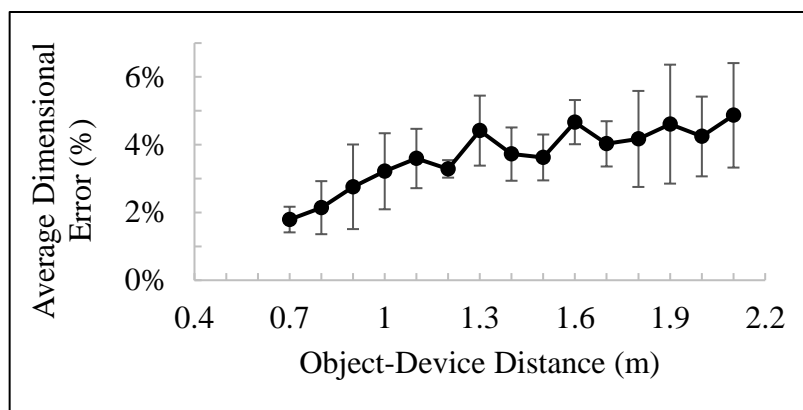


Figure 5.8 Influence of low lighting (7 lux-30 lux) on the average dimensional error for point cloud models generated by ZED Camera

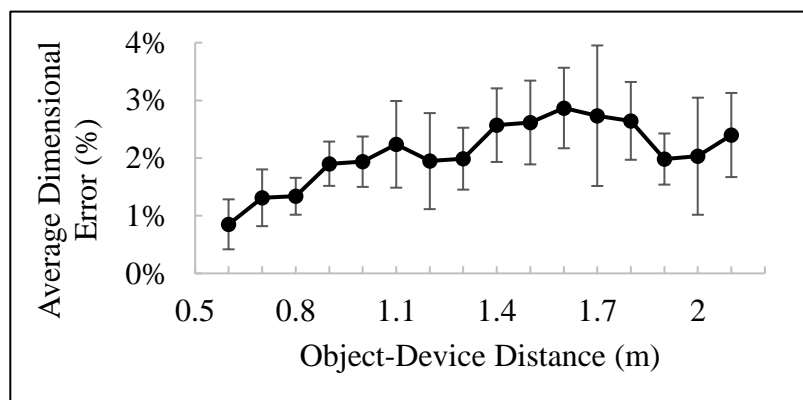


Figure 5.9 Influence of low lighting (7 lux-30 lux) on the average dimensional error for point cloud models generated by Tango

It was observed that ZED camera as-built models had lesser dimensional errors with better illumination (Figure 5.8). On the other hand, the average dimensional error of both the devices in high light condition is shown in Figure 5.10 and Figure 5.11. It was observed that higher illumination interferes with infrared technology causing

dimensional errors in as-built models generated by Tango (Figure 5.11). Thus, the dimensional error increased marginally in this lighting range. Hence, it can be used reliably during daytime and night-time provided there is minimum illumination, but less concentrated light. But during periods of high infrared radiation such as noon and evening, Tango can experience interference in its capturing technology, thus affecting the quality of as-built models. The IR camera also prevents Tango from being used outdoors under direct sunlight. This affects the capture of exteriors sections of buildings.

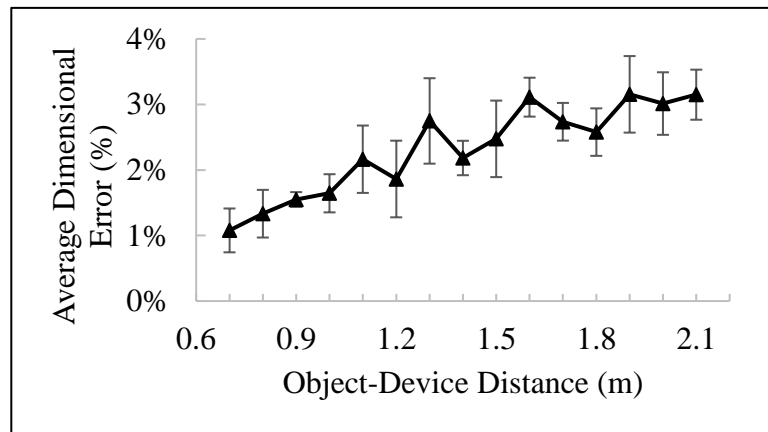


Figure 5.10 Influence of high lighting (170 lux – 230 lux) on the average dimensional error for point cloud models generated by ZED Camera

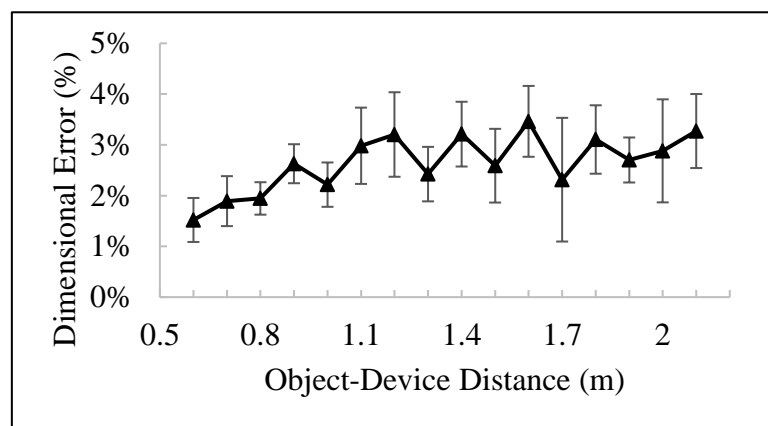


Figure 5.11 Influence of high lighting (170lux-230lux) on the dimensional error for point cloud models generated by Tango

Further, it should be noted that the variation observed in the dimensional error under the two lighting conditions is marginal. However, the variation between of average dimensional error between the datasets is high for Tango in the high light condition (Figure 5.9 and Figure 5.11). A similar variation was observed for ZED in the low light

variation (Figure 5.8). One of the reasons for this variation in the dimensional error across the sample is the optimization process embedded in the SDK.

5.3 PHASE 1: PERFORMANCE EVALUATION IN CONSTRUCTION SITE

5.3.1 Accuracy of as-built models

The percentage of dimensional error for as-built models generated from the construction site was calculated. The results are shown in Table 5.1. In each construction stage, different components' dimensions were measured. The components B1, B2, B3, B4, B5, and B6 indicate the length of six different beams. The components C1, C2, C3, C4, C5 and C6 indicate heights of six different columns. The Tango tablet has an average dimensional error of 3.07% and ZED has 7.81%.

Table 5.1 Accuracy of as-built model from construction site

Element Description	Actual Dimensions (m)	Tango: As-Built Dimensions (m)	ZED: As-Built Dimensions (m)	Tango: Dimensional Error (m)	ZED: Dimensional Error (m)
Stage 1: Component B1	5.8	5.74	5.31	1.03%	8.45%
Stage 1: Component B2	4	3.96	3.85	1.00%	3.75%
Stage 1: Component C1	3.05	3.07	2.75	0.66%	9.84%
Stage1: Component C2	3.05	3.08	2.77	0.98%	9.18%
Stage 2: Component B3	3.5	3.41	3.18	2.57%	9.14%
Stage2: Component B4	4	3.92	3.72	2.00%	7.00%
Stage 2: Component C3	3.05	3.1	2.92	1.64%	4.26%
Stage 2: Component C4	3.05	3.12	3.03	2.30%	0.66%
Stage3: Component B5	4.3	4.56	3.63	6.05%	15.58%
Stage 3: Component B6	3.5	3.41	3.1	2.57%	11.43%
Stage3: Component C5	3.05	2.91	2.87	4.59%	5.90%
Stage 3: Component C6	3.05	2.89	2.75	5.25%	9.84%
Stage4: Component B5	4.3	3.97	3.81	7.67%	11.40%
Stage 4: Component B6	3.5	3.35	3.16	4.29%	9.71%
Stage 4: Component C5	3.05	2.95	2.95	3.28%	3.28%
Stage 4: Component C6	3.05	2.95	2.88	3.28%	5.57%
Average Dimensional Error (%)				3.07%	7.81%

In comparison, the point clouds generated by laser scanners have a dimensional error in the range of 0.004-0.009m with a higher resolution (Golparvar-Fard et al. 2011c). Hence, both ZED and Tango can be used for progress monitoring applications. However, due to a higher dimensional error and lower resolution, they can only be used for capturing large components such as masonry and concreting elements. Smaller components such as MEP elements, reinforcements, fixtures could not be captured for this research. Hence, the feasibility of using the devices for assessing progress for these components was not studied.

Tango tablet was observed to have more accurate as-built models when compared to ZED camera due to its active sensor based method (ToF) for depth computation.

5.3.2 Mobility and time efficiency

The ZED camera weighs 160 grams, making it very light to carry and use. However, to scan an area, the camera needs to be powered through a USB cable to a computer that runs the SDK. Thus, the user needs to carry a computer in order to use the device on site. Tango, on the other hand, weighs 370g and does not require an external power source. The point cloud is generated by the Application can be viewed in real time on the tablet, making it much more user-friendly. To determine the time efficiency of the device, the time required for preparation, scanning, and data processing are measured for the four stages.

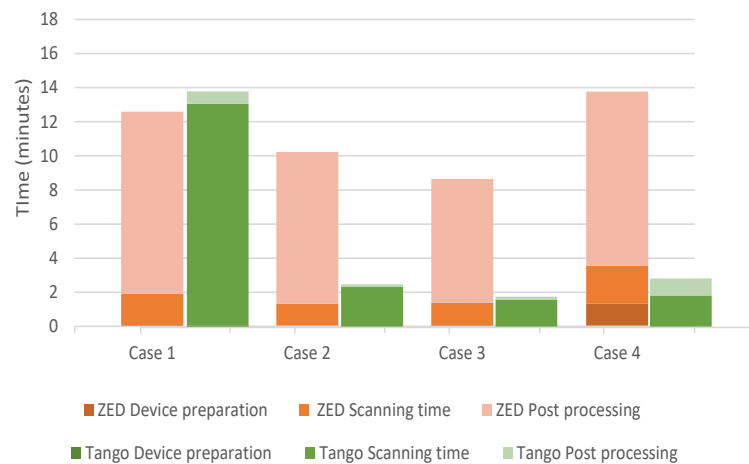


Figure 5.12 Comparison of Scanning times for construction site

From the Figure 5.12, the pre-processing/device preparation prior to the scanning process is negligible for both the devices. While the post-processing time of ZED is higher than tango for as-built data from all the construction stages, it is more stable for prolonged use. Since ZED requires an external power supply for operation, workarounds using processor boards such as NVidia Jetson kits help ease the mobility. ZED camera, with its long-range capacity, can be used to capture both small and large areas without experiencing malfunctions.

As noted in section 5.2.3, the FOV of ZED is higher than that of Tango. This influences the speed of capture in construction sites where multiple areas needed to be scanned continuously. Prolonged use of the Tango tablet results in heating of device and

crashing of either the scanning app/sensor/ OS. This results in loss of scan data that cannot be retrieved even upon restarting the device. Thus, Tango cannot be used continuously to scan multiple areas in a site due to hardware and software limitations.

5.3.3 Influence of lighting conditions

Stereo reconstruction algorithms depend on accurate correspondence of the image frames, which in turn relies on unique features in the images. These features are better identified with enhanced lighting conditions. Therefore, lighting indirectly influences the quality of the stereo-based 3D reconstruction. It was observed that multiple surfaces were reconstructed for areas which were illuminated with concentrated light in both ZED camera and Tango during rescanning. Figure 5.13(a) is a representative image of an area of masonry wall while Figure 5.13 (b) shows distortions in as-built point cloud model generated by ZED camera due to rescanning.

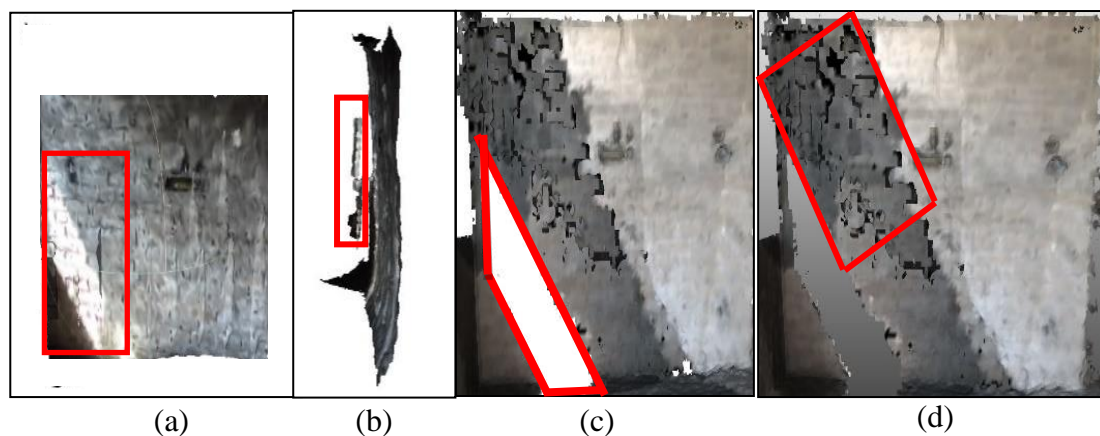


Figure 5.13 (a) Original masonry wall with area of interest highlighted in red; (b) Side view of point cloud from ZED: Highlighted area shows multiple surface reconstructed due to rescanning; (c) Front view of point cloud from Tango: Highlighted area shows loss of data due to sunlight interference; (d) Front view of Point cloud from Tango: Highlighted area shows distortion due to rescanning

The Tango tablet uses Infrared light to detect the depth of the scene. As a result, any object directly illuminated by sunlight or artificial lighting was not captured (Figure 5.13(c)). Objects with illumination less than 4 Lux were either not detected by Tango's IR sensor or the resulting reconstruction was distorted. Rescanning also causes significant problems such as generation of multiple surfaces instead of one surface (Figure 5.13 (d)).

For both the devices, rescanning causes distortions in reconstruction. However, during the usage in construction environments, some areas might not be captured due to

occlusions. This can result in attempts of user to rescan. Consequently, localization errors occur, which results in the erroneous reconstruction of multiple surfaces for the same object. Thus, a path plan based on scanning environment is necessary to avoid rescanning.

5.3.4 Device characteristics

The FoV of the device and the maximum range of the device directly influence the scanning path. ZED's horizontal FOV is significantly larger than its vertical FoV and its maximum range is 20m from the specification (Stereolabs 2016). Hence, the ZED camera was rotated 90° horizontally. This helped capture a larger area vertically. Because of the limited range of Tango, adopting a 90° horizontal flip did not cover more scan area.

The angular speed of ZED camera for scanning was limited to 0.2m/s-0.5m/s and for Tango was limited to 0.5-1m/s. With the increase in this speed, both devices lose track of its localization, causing drift errors. Thus, field personnel needs to be able to capture the scene with a constant speed within the above range to avoid loss of data.

5.4 PHASE 3: PROGRESS RECOGNITION SYSTEM EVALUATION

Three configurations (Figure 5.14 (a), (b) and (c)) in the laboratory test bed were captured using both ZED camera and Tango tablet. The as-built models generated were used to test the efficiency of the progress recognition system. The configurations are shown in Figure 5.14 (a), (b) and (c). The as-built model was given as input to the progress recognition system along with the BIM model of the configuration. The resulting model after 'voxel occupancy comparison' is shown in Figure 5.14 (g), (h) and (i).

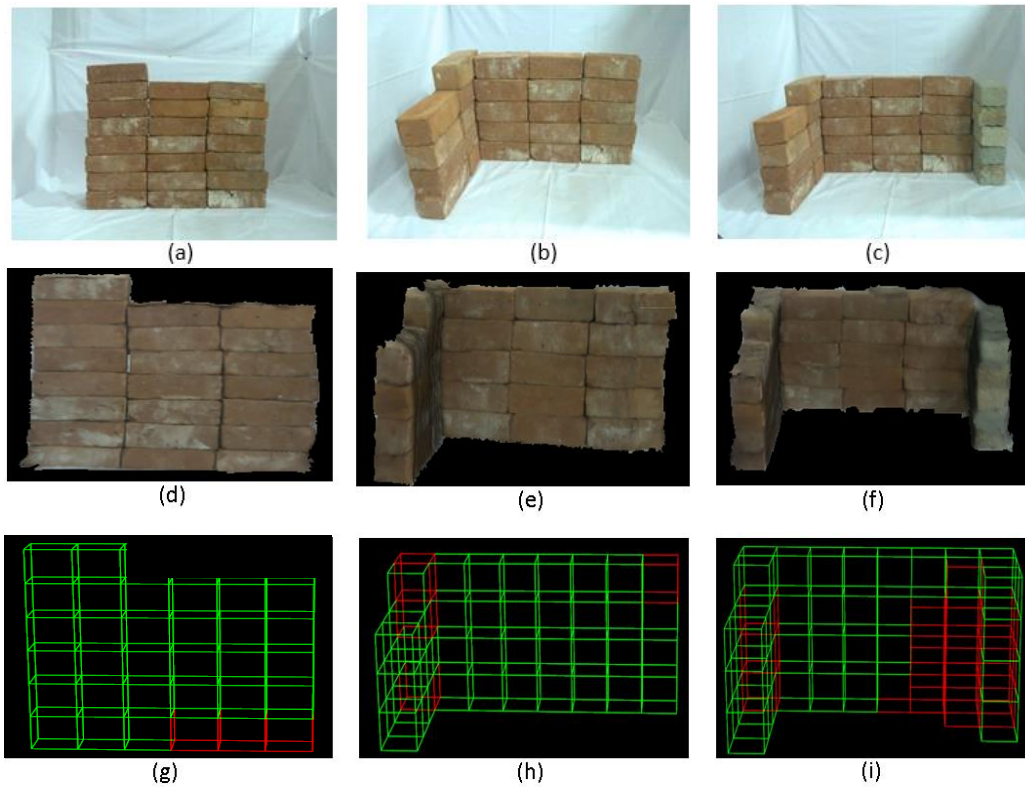


Figure 5.14 (a), (b), (c) Laboratory configurations; (d), (e), (f) Point clouds generated from Tango; (g), (h), (i) Results of progress recognition system: classification legend -green voxels indicate correctly classified voxels, red voxels indicate wrongly classified voxels

The as-planned BIM model of the stage no. 3 in the construction site is shown in Figure 5.15 (a), with the as-built point cloud model from ZED camera shown in Figure 5.15 (b). The resulting model after ‘voxel occupancy comparison’ is shown in Figure 5.15 (c).

In Figure 5.14 and Figure 5.15, the green voxels indicate voxels that were classified as occupied in both the as-built and as-planned model and thus classified as ‘built’. The red indicates the voxels misclassified (False Positive or False Negative). Table 5.2

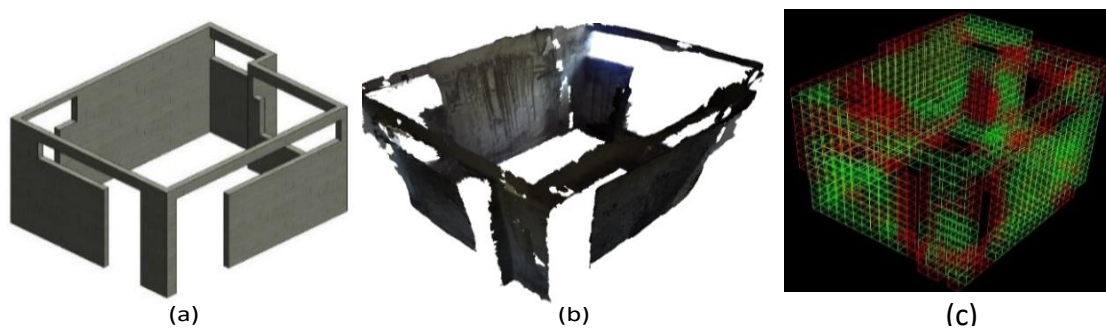


Figure 5.15 (a) BIM of construction stage 3; (b) As-built point cloud model generated by Tango for construction stage 3; (c) Voxel based binary classifier: green voxels indicate “built” voxel & red indicate ‘not-built’

shows the voxel colour legend for the progress recognised using the workflow shown in Figure 4.8. In the table below, A_i and B_i indicate the voxel occupancy of the as-built model and voxel occupancy of the as-planned model respectively.

The green voxels indicate voxels that were classified correctly (True Positive) and thus classified as ‘built’. The red voxels indicate the voxels misclassified (False Positive or False Negative). The accuracy of the as-built data from both the devices is represented in Figure 5.16.

Table 5.2 Voxel colour for progress recognition

Voxel Occupancy Comparison	Inference	Construction Status	Voxel Color
$A_i=TRUE \ \& \ B_i=TRUE$	Correct Classification	Built	Green
$A_i=TRUE \ \& \ B_i=FALSE$	Wrong Classification	Built in Advance/ Incorrect construction	Red
$A_i=FALSE \ \& \ B_i=TRUE$	Wrong Classification	Not Built	Red
$A_i=FALSE \ \& \ B_i=FALSE$	Correct Classification	-	Black

The accuracy of the ‘built’ voxels is assessed through confusion matrix metrics as explained in Section 4.3.2. The classifier predicts with an average accuracy of 91.62% accuracy with an average recall rate of 74.61% and an average precision of 97.16% for as-built data from ZED camera in the laboratory test bed. For as-built data from Tango tablet in laboratory test bed, the average accuracy of prediction is 94.10% accuracy with an average recall rate of 75.55% and an average precision of 91.36%. But, the accuracy of progress measurement of as-built data from the construction site is lesser than the laboratory test data (Figure 5.16). It was observed that the Recall and Precision values decreased with increase in model complexity in the laboratory test bed.

Lower recall values can be attributed to the loss of data/gaps in the model due to poor 3D reconstruction which increases the number of False Negatives (FN). On the other hand, lower precision is caused by a higher number of False Positives (FP). This can be due to distortion of point cloud due to lighting conditions and accuracy limitations. Loss of data due to occlusions, lesser resolution due to improper scanning technique, error in ICP registration have an effect on the final accuracy of the progress recognition system.

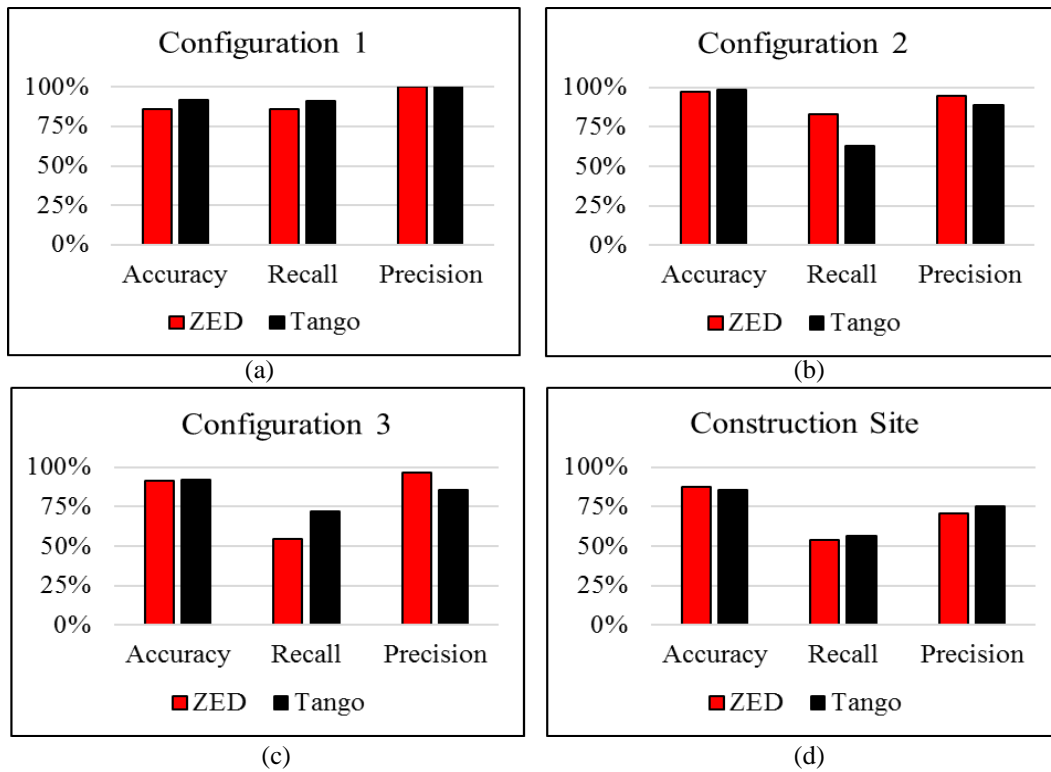


Figure 5.16 Accuracy, precision, and recall values for as-built data from ZED camera and Tango (a) Laboratory configuration1 (b) Laboratory configuration 2 (c) Laboratory configuration 3 (d) Construction site

Further, the recall of as-built data from Tango reduces sharply with increase in a number of planes in the model, but the precision is greater than 75% for all cases. ZED camera's as-built data shows a higher average recall, with a reduced precision. Conventionally, lower FN and FP values indicate better prediction confidence. However, for construction monitoring purposes, a lower recall value with higher precision is preferable, since all elements which are classified as 'built' can be trusted with a higher confidence. Also, in the context of productivity, this progress recognition system always predicts conservatively, thus avoiding optimistic rates.

The prediction accuracies achieved by this system depends on the quality of the point cloud given as input. The performance evaluation tests in the laboratory environment give a yardstick for optimum values obtainable under near-ideal conditions. For achieving the optimum quality of the as-built data, the devices need to be used based on the threshold ranges determined in laboratory experiments of this study. These conditions cannot be reproducible in a construction site. Thus, the as-built data from the construction site gives a better insight on the performance of the data for progress monitoring applications. Loss of data due to occlusions, lesser resolution due to

improper scanning technique, and error in ICP registration have an effect on the final accuracy of the progress recognition system.

Additionally, the computation time for the system to recognise the progress was less than 5 minutes for the as-built model from the construction site which was the largest model evaluated in this study. Hence, the prototype developed in this system is time efficient.

5.4.1 Comparison between stereovision and infrared range imaging devices

ZED camera, as noted before is a passive sensor which uses stereo images for 3D reconstruction. Tango is an active sensor which uses Infrared rays for depth perception and 3D reconstruction. It was observed that the as-built models generated by both the devices showed comparable progress recognition accuracies in laboratory test bed and in the construction site despite ZED camera’s point cloud having lower accuracy.

5.4.2 Comparison with other progress recognition methodologies

To ascertain the quality of the as-built data from range images against data from other technologies, comparisons with progress recognition values from research works, which used other classifiers, were made. Figure 5.17 shows the comparison of the level of accuracy achieved using as-built data from ZED and Tango against laser, conventional Single Camera photogrammetry, and Stereo Photogrammetry.

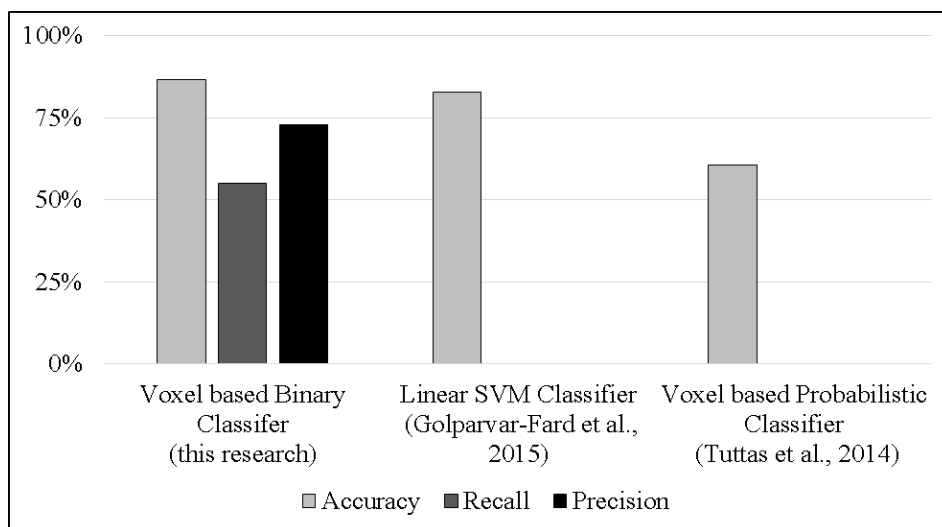


Figure 5.17 Performance of classifiers for as-built data from range cameras

Due to gaps in reported values in literature, a complete set of accuracy, recall, and precision are not shown. From the figure, it was observed that the voxel-based binary classifier used in this research showed a higher accuracy, precision and recall values compared to linear SVM classifier which uses as-built models from stereo photogrammetry. Further, the classifier also performs better compared to the voxel-based probabilistic classifier developed by Tuttas et al. which uses mono photogrammetry. However, it should be noted that even though mono and stereo photogrammetry fall under range imaging devices, the camera specification, method of capture and post-processing will influence the performance of the classifier. Hence, the above comparison can be used only as a reference.

5.4.3 Comparison with other technologies

Further to the above comparisons, the progress recognition of the as-built data from the range imaging devices was compared to conventional technologies such as lasers, mono photogrammetry and stereo photogrammetry as shown in Figure 5.18.

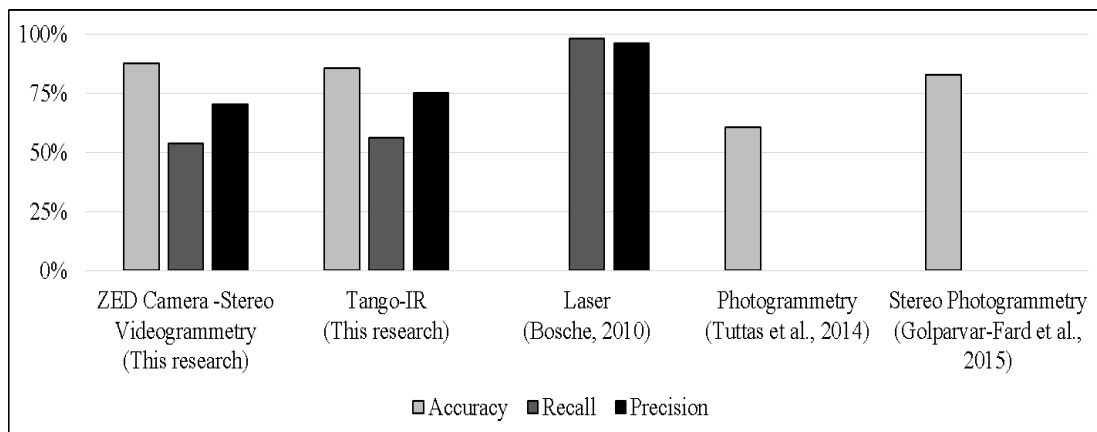


Figure 5.18 Comparison of confusion matrix metrics for progress recognition using as-built models generated by ZED and Tango against other technologies

Due to gaps in reported values in literature, a complete set of accuracy, recall, and precision are not shown. The progress prediction accuracy using as-built data generated by both ZED stereo camera and Tango tablet is higher than conventional methodologies using as-built data from similar technology such as photogrammetry. However, the recall and precision levels achievable are lesser than that of as-built data from Lasers. The above comparison does not take into account the capabilities of the classifier in handling low quality data. Consequently, these figures provide only an approximate comparison.

5.5 SUMMARY

This chapter elaborates on the results of the performance evaluation experiments for as-built models generated by both the reality capture devices. Both the devices were used to capture reality in a laboratory test bed setup and in construction site. The optimum range of usage, stability of the device in a construction site, the accuracy of the as-built models generated, the time efficiency of the devices and influence of external factors such as lighting were studied and the optimum values were established which can aid as best practices for usage of these devices. The as-built models generated in both the environments were used to evaluate the efficiency of the progress recognition system. Object Recognition metrics such as Accuracy, Recall, and Precision were used to evaluate the efficiency of the system that was then compared with efficiencies of other methods from the literature. The voxel based binary classifier based progress recognition system used in this research showed a higher prediction accuracy compared to other methods which use as-built data from similar technologies.

CHAPTER 6

SUMMARY AND CONCLUSION

This chapter summarizes the work done in this research. Conclusions from the work and the contributions of the work are present here. The potential for further work in this area and a brief introduction to extended applications of this framework are also presented.

6.1 SUMMARY

This research focused on the evaluation of two devices that use two different technologies: a passive stereovision camera and an active infrared device in construction environments to generate as-built models. An automated data capture system consisting of both the technologies was adopted to test the viability of using them for capturing as-built data. An automated monitoring system was adopted over the traditional monitoring system to monitor the progress as the automated monitoring system performs better in terms of accuracy and response time. This study explored the type of experiments needed to be performed to evaluate the applicability of these devices in construction environments that are dynamic and complex.

Chapter 1 introduced the need for automated progress monitoring along with the research question. Chapter 2 reviewed the existing literature in the area of technologies for construction progress monitoring. These included lasers, RFID, barcodes, GPS/GIS, and imaging based sensors. It also reviewed the prior works on evaluation parameters for such technologies and point cloud data. Finally, the various methods for progress recognition were reviewed. The chapter concluded with a discussion on the research gaps identified from the literature review.

Based on the identified research gap, the problem statement, aim, objectives and scope of work were defined in chapter 3. This was followed by an overview of the research methodology adopted. The methodology is split into three phases with a discussion on the details of each phase. Phase 1 consisted of evaluation of the range imaging devices based on the literature review done in chapter 2. Phase 2 focussed on the design of the automated progress recognition system and the development of a prototype. In phase 3,

the developed prototype is evaluated for progress recognition accuracy. A brief introduction to the scan-to-BIM registration process was also given.

In chapter 4, the range imaging devices evaluated in this study were introduced. Additionally, the software platforms for performance evaluation, the testing environment such as laboratory test bed and construction site were discussed. The experimental tests for the performance evaluation of the devices were elaborated. Further, the design and prototype development of the automated progress recognition system was elaborated. The metrics for evaluating the prototype for progress recognition were also discussed.

Chapter 5 presented the results of the all the performance evaluation tests of Phase 1 along with corresponding discussions of their implication for construction. Further, section 5.4 on phase 3 presented the performance of the progress recognition system based on accuracy, precision, and recall metrics. The values for the metrics obtained in this study were compared with other progress recognition methods. Further, a comparison of performance of range imaging technologies against other technologies such as lasers, conventional photogrammetry for progress recognition was presented. These comparisons were used to prove the feasibility of the range imaging devices for construction progress monitoring.

Finally, the conclusions from this study along with the theoretical and practical contributions are presented in Chapter 6. Further, the limitations of this work in terms of scope, and methodologies adopted are discussed. A brief discussion on the potential areas for future work are discussed.

6.2 CONCLUSIONS

This study explored the application of commercially available range imaging device for assessing construction progress. The feasibility of using the as-built data from both the active infrared and passive stereovision range imaging devices for construction progress monitoring was explored. The voxel-based binary classifier developed for detecting progress showed an average accuracy of 92% accuracy for laboratory test bed and 86% accuracy for construction site data. This answers the main research question of this work.

The stereovision device was observed to be more suitable for general construction applications in which the level of detail of capture is minimal and accuracy is not a determining factor. Its long range of operation, higher stability during capture and passive sensor based depth perception enable it to be used for capturing both interiors and exteriors of the construction.

A summary of the performance evaluation test results and the corresponding implication for construction is tabulated in Table 6.1.

Table 6.1 Summary of performance evaluation tests

Parameters	Passive Stereovision device: ZED	Active infrared device: Tango	Implication for Construction
Accuracy of Point Clouds	Laboratory: 1.4 cm error for every 1m Construction site: Average error of 8cm for every 1m	Laboratory: 1cm error for every 1m Construction site: Average error of 3cm for every 1m	Stereovision and IR range imaging devices can be used for capturing large elements and assessing its construction progress with the present hardware and software configurations
Optimum Range of Operation	0.7-1m	0.6-1m	Requires user to plan scan path to accommodate the range.
Mobility	Lightweight. Powered by laptop/computer	Lightweight. Constant use after 30-40 minutes causes heating of device	Passive stereovision devices suitable for scanning large construction sites requiring multiple scans consecutively. Active IR devices can be used for smaller areas only
Time Efficiency	Large FOV. Lower scanning time. Higher post processing time	Small FOV. Higher Scanning Time. Lower post processing time	
Influence of Lighting Conditions	Additional illumination for scanning	Sunlight Interference causes distortions and improper reconstruction	Stereovision devices usage: during daytime only and to capture indoors and outdoors. IR devices usage: Building Exteriors cannot be captured during daytime
Device Stability	Lower probability of data corruption	Overheating causes crashes, loss of data	Stereovision devices have higher reliability in for on site usage

- Active sensors for depth perception are more suitable for applications requiring higher accuracy and involving capture of indoor areas.

- The performance evaluation tests in the laboratory test bed provide a point of reference for optimum values obtainable under near-ideal conditions.
- As-built data generated by passive stereovision device in laboratory test showed a progress recognition accuracy of 91.62% and 87.54% for the construction site.
- As-built data generated by active infrared device showed a progress prediction accuracy of 94.51% for laboratory test bed and 85.62% for the Construction site.
- The as-built data from the active IR device in laboratory test bed shows a marginally higher Recall and Precision for progress prediction.
- Stereovision and Infrared devices, despite accuracy and range limitations, were determined to be viable for construction progress monitoring.

Both the range imaging devices used in this study have costs under \$500. Their advantages like ease of use, higher mobility, quick scanning time, low post processing and quality of as-built data, make them cost-effective solutions for construction progress monitoring applications. However, there are some limitations. The passive stereovision videogrammetry device used in this research faces corruption in data when there is an interference due to movement of objects in a scene. This can lead to loss of data, especially in a construction site where the environment is subject to constant movement of men and machinery. Further, the progress measurement system developed in this research does not take into account the occlusions in the captured as-built model. As a result, the onus is on the user to ensure the entire scene is captured. Errors in scan-to-BIM registration decrease the overall efficiency of the progress recognition system. Further, gaps in the point cloud model due to errors in reconstruction results in higher misclassification rate, resulting in poor performance of the classifier and the as-built data.

In this study, the range imaging devices were used to capture only large construction elements such as masonry walls, concrete beams, floors and columns. Interior components such as tiles, finishes, paint, electrical components, and plumbing fixtures could not be captured accurately due to low point cloud resolution. As a result, the level of monitoring using these devices will be restricted. However, in a typical building projects, more than 50% of activities are based on concreting and masonry elements

(Navon 2005). Hence, for a macro level monitoring, progress assessment of the activities can help in project control. Future improvements in hardware and software can increase the range of elements being captured which can further extend the use of these devices for micro level monitoring.

6.3 THEORETICAL CONTRIBUTIONS

This study assessed the feasibility of using range imaging devices for capturing as-built construction for progress monitoring applications. The main contributions from this study are listed below:

- Assessment of influencing parameters for Stereovision and Infrared technologies for performance for construction applications
- Determination of best practices for optimum usage of both technologies through controlled environment studies
- Development of automated progress recognition system and validation with data from controlled environment and uncontrolled environment

6.3.1 Evaluation of range imaging for construction progress monitoring

A primary driver behind this study was the fact that very little data existed that could help to understand the parameters to be considered for assessing the viability of technologies for construction progress monitoring applications. While accuracy has been extensively studied for many technologies, factors such as time efficiency, device characteristics, operating range of the devices, and lighting conditions have not been studied.

ZED camera and Google Tango are chosen as representative cases for passive stereovision and active infrared technologies respectively. While the hardware and software is expected to evolve, the underlying technology will remain the same. The methodology for experimental evaluation of these parameters in this work helps to fill the gap in the existing knowledge in selection of technology for construction applications. Additionally it can be used for evaluating other active and passive range imaging devices.

In this research, parameters that were important from a construction perspective were selected for the performance evaluation. The study showed that the range imaging

devices were time efficient, but possess technical limitations such as lower battery life, speed of capture etc. Evaluation of the devices for these qualitative factors will help to understand the practical viability of using them on the construction site.

6.3.2 Comparison between passive and active range imaging devices

While research works exploring commercially available range imaging devices exist, there is no research in comparison of range imaging devices using different techniques for depth perception. In this research, Google[®] Tango is a range imaging device which uses active infrared sensor and Time of Flight (ToF) technique for depth perception. On the other hand, ZED camera uses passive stereo vision for depth computation. Prior research works have studied the performance in terms of accuracy, resolution of the devices using similar technology based on active sensors and depth sensing mechanism such as KINECT, XTion PRO, and to some extent Google Tango as elaborated in the literature review section. However, the performance of commercially available range imaging devices for construction progress monitoring have not been studied. In particular, passive range imaging devices do not have any established benchmarks for accuracy and progress recognition. The performance evaluation of the passive stereovision ZED camera in this study fills the above gap to an extent.

Further, this research provides a ground base for comparison of active and passive range imaging devices in terms of performance of the device for construction application. The progress recognition accuracies using the as-built data from both the devices showed negligible variation. Hence, while the accuracy of the point clouds from both these devices vary, both the devices can still be used for progress monitoring applications. However, the level of detail of the progress monitoring is limited due to their accuracy and resolution limitations. This will be elaborated in the upcoming sections.

6.4 PRACTICAL CONTRIBUTIONS

6.4.1 Development of automated progress recognition system

The practical contribution of this research is the prototype of the automated progress recognition system. The system uses three input parameters: BIM, as-built point cloud model, and threshold values, for recognizing the progress. The total time for progress recognition using the data obtained from the construction site was under 5 minutes. Hence, the prototype assesses the progress quickly and automatically. This is of

relevance to construction, where progress updates are required frequently. A time-efficient progress recognition system accommodates shorter frequency of updates such as daily/weekly/biweekly.

6.5 LIMITATIONS AND FUTURE WORK

A limitation of this study is that factors, like uncertainties in capturing a scene of interest completely, errors in reconstruction, errors in scan-to-BIM registration, decrease the overall efficiency of the progress detection system. Further, occlusions and gaps in the point cloud model due to errors in reconstruction results in higher misclassification rate, resulting in poor performance of the classifier and the as-built data. Since the resolution and the dimensional accuracy of both the range imaging devices are low, smaller components such as plumbing and electrical fixtures, reinforcements, HVAC ducts will not be captured accurately. However, it is expected that with the evolution of the technology, the hardware can potentially be able to detect these components in future.

In keeping with the big picture of the research, only some performance evaluation parameters were studied. Further parameters such as the effect of additional external lighting, object characteristics etc. can be potential future areas of research. In the below sections, such prospective areas are briefly discussed.

6.5.1 Extension of current research

The research in automated progress monitoring using technologies has increasingly found more importance due to the availability of better technological capabilities and increasing processing powers of devices. However, there are still processes in which human intervention is necessary. The progress recognition workflow developed in this study aims to automate the monitoring system to an extent where it can be used with minimal user interventions. However, with advancements in hardware capabilities, more automation and better accuracy can be achieved. Some of the directions for future work are summarized below.

- Assessment of applicability of technologies for other construction activities such as earthwork, MEP, reinforcement
- Extension of the current progress recognition system to handle missing data and Occlusion
- Implementing heuristics and rule based checking to overcome missing data

6.5.2 Other areas

Considering that the technology has not yet reached maturity, there are numerous areas that can be worked upon in future. Some of them are discussed below.

- Extension of progress recognition system to include conversion of measured progress to IFC, for integrating and updating BIM automatically
- Visualization of the updated schedule along with BIM in BIM platforms
- Remote drone based automated as-built data collection using ZED and Tango. This involves research on path planning for efficient capture, real-time transmission, and processing of data for visualization
- Extension of progress recognition system to determine the quantity of component completed, which can be used for quality conformance checks.

This study explored the feasibility of using these range imaging technologies for one construction site. More case studies in the field can help accurate documentation of the performance of these technologies. Additionally, more elaborate laboratory experimental evaluations with the inclusion of other parameters such as intensity of lighting, the influence of object texture, the orientation of the device can help gain insights into the performance of these devices. These evaluations can also be extended towards establishing benchmarks and best practices for using these devices in construction applications.

REFERENCES

- Burbano, A., Vasiliu, M., and Bouaziz, S. 2016 '3D Cameras Benchmark for Human Tracking in Hybrid Distributed Smart Camera Networks'. *Proceedings of the 10th International Conference on Distributed Smart Camera - '16*, 76–83.
- Schöps, T., Sattler, T., Häne, C., and Pollefeys, M. 2016 'Large-scale outdoor 3D reconstruction on a mobile device'. *Computer Vision and Image Understanding*, 157, 151–166.
- Ishida, K. 2016 'Construction Progress Management and Interior Work Analysis Using Kinect 3D Image Sensors'. *Proc. of 33rd International Symposium on Automation and Robotics in Construction*, Auburn, AL, USA, 314–322.
- Froehlich, M., and Azhar, S. 2016 'Handheld Simultaneous Localization and Mapping Devices for 3D Scanning'. *Proceedings of the 33rd Int. Symp. Autom. Robot. Constr.*, 975–984.
- Braun, A., Borrmann, A., Tuttas, S., and Stilla, U. 2016 'Classification of detection states in construction progress monitoring'. *eWork and eBusiness in Architecture, Engineering and Construction*, 473–480.
- Stereolabs. 2016 'ZED - Depth Sensing and Camera Tracking'. <<https://www.stereolabs.com/zed/specs/>> (Sep. 11, 2017).
- Kopsida, M., Brilakis, I., and Vela, P. 2015 'A Review of Automated Construction Progress and Inspection Methods'. *Proceedings of the 32nd CIB W78 Conference on Construction IT*, 421–431.
- Valero, E., Adán, A., and Cerrada, C. 2015 'Evolution of RFID Applications in Construction: A Literature Review'. *Sensors*, 15(7), 15988–16008.
- Braun, A., Tuttas, S., Borrmann, A., and Stilla, U. 2015 'A concept for automated construction progress monitoring using BIM-based geometric constraints and photogrammetric point clouds'. *Journal of Information Technology in Construction*, 20, 68–79.
- Zennaro, S., Munaro, M., Milani, S., Zanuttigh, P., Bernardi, A., Ghidoni, S., and Menegatti, E. 2015 'Performance evaluation of the 1st and 2nd generation Kinect for multimedia applications'. *Proceedings of IEEE International Conference on Multimedia and Expo*, 1–6.
- Pătrăucean, V., Armeni, I., Nahangi, M., Yeung, J., Brilakis, I., and Haas, C. 2015 'State of research in automatic as-built modelling'. *Advanced Engineering Informatics*, 29, 162–171.
- Golparvar-Fard, M., Peña-Mora, F., and Savarese, S. 2015 'Automated Progress Monitoring Using Unordered Daily Construction Photographs and IFC-Based Building Information Models'. *Journal of Computing in Civil Engineering*, 29(1), 147.
- Daniel GM. 2015 'Alignment and Registration - CloudCompareWiki'. *Version 2*,

<http://www.cloudcompare.org/doc/wiki/index.php?title=Alignment_and_Regist ration> (May 28, 2017).

- Han, K. K., Cline, D., and Golparvar-Fard, M. 2015 'Formalized knowledge of construction sequencing for visual monitoring of work-in-progress via incomplete point clouds and low-LoD 4D BIMs'. *Advanced Engineering Informatics*, 29, 889–901.
- Sirmacek, B., and Lindenbergh, R. 2014 'Accuracy assessment of building point clouds automatically generated from iphone images'. *International Archives of the Photogrammetry, Remote Sensing and Spatial Information Sciences - ISPRS Archives*, 547–552.
- Tuttas, S., Braun, A., Borrmann, A., and Stilla, U. 2014 'Comparison of photogrammetric point clouds with BIM building elements for construction progress monitoring'. *International Archives of the Photogrammetry, Remote Sensing and Spatial Information Sciences - ISPRS Archives*, 40(3), 341–345.
- Dimitrov, A., and Golparvar-Fard, M. 2014 'Vision-based material recognition for automated monitoring of construction progress and generating building information modeling from unordered site image collections'. *Advanced Engineering Informatics*, 28(1), 37–49.
- Vähä, P., Heikkilä, T., Kilpeläinen, P., Järviluoma, M., and Gambao, E. 2013 'Extending automation of building construction - Survey on potential sensor technologies and robotic applications'. *Automation in Construction*, Elsevier B.V., 36, 168–178.
- Ikonen, J., Knutas, A., Hämäläinen, H., Ihonen, M., Porras, J., and Kallonen, T. 2013 'Use of embedded RFID tags in concrete element supply chains'. *Journal of Information Technology in Construction*, 18(April), 119–147.
- Wang, X., Love, P. E. D., Kim, M. J., Park, C.-S., Sing, C.-P., and Hou, L. 2013 'A conceptual framework for integrating building information modeling with augmented reality'. *Automation in Construction*, Elsevier B.V., 34, 37–44.
- Pradhananga, N., and Teizer, J. 2013 'Automatic spatio-temporal analysis of construction site equipment operations using GPS data'. *Automation in Construction*, Elsevier B.V., 29, 107–122.
- Zhang, C., and Arditi, D. 2013 'Automated progress control using laser scanning technology'. *Automation in Construction*, 36, 108–116.
- Kim, J. Y., and Caldas, C. H. 2013 'Vision-based action recognition in the internal construction site using interactions between worker actions and construction objects'. *Proc. of 30th Int. Symp. Autom. Robot. Constr.*, 661–668.
- Naticchia, B., Vaccarini, M., and Carbonari, A. 2013 'A monitoring system for real-time interference control on large construction sites'. *Automation in Construction*, Elsevier B.V., 29, 148–160.
- Hui, L. and Brilakis, I. 2013 'Real-Time Bricks Counting for Construction Progress Monitoring'. *Proceedings of the 2013 ASCE International Workshop on*

Computing in Civil Engineering, (November), 818–824.

- Golparvar Fard, M., Peña Mora, F., Savarese, S., Golparvar-fard, M., Peña Mora, F., and Savarese, S. 2012 ‘Automated Progress Monitoring Using Unordered Daily Construction Photographs and IFC-Based Building Information Models’. *Journal of Computing in Civil Engineering*, 29(1), 147.
- Bhatla, A., Choe, S. Y., Fierro, O., and Leite, F. 2012 ‘Evaluation of accuracy of as-built 3D modeling from photos taken by handheld digital cameras’. *Automation in Construction*, 28(May), 116–127.
- Weerasinghe, I. P. T., Ruwanpura, J. Y., Boyd, J. E., and Habib, A. F. 2012 ‘Application of Microsoft Kinect Sensor for Tracking Construction Workers’. *Proc. of Construction Research Congress 2012*, American Society of Civil Engineers, Reston, VA, 858–867.
- Rafibakhsh, N., Gong, J., Siddiqui, M. K., Gordon, C., and Lee, H. F. 2012 ‘Analysis of XBOX Kinect Sensor Data for Use on Construction Sites : Depth Accuracy and Sensor Interference Assessment’. *Proc. of Construction Research Congress 2012*, 848–857.
- Nicolas, F., Turkan, Y., Bosche, F., Haas, C. T., and Haas, R. 2012 ‘Automated progress tracking using 4D schedule and 3D sensing technologies’. *Automation in Construction*, 22, 414–421.
- Golparvar-Fard, M., Bohn, J., Teizer, J., Savarese, S., and Peña-Mora, F. 2011a ‘Evaluation of image-based modeling and laser scanning accuracy for emerging automated performance monitoring techniques’. *Automation in Construction*, 20(8), 1143–1155.
- Cheng, T., Venugopal, M., Teizer, J., and Vela, P. A. 2011 ‘Performance evaluation of ultra wideband technology for construction resource location tracking in harsh environments’. *Automation in Construction*, 20(8), 1173–1184.
- Brilakis, I., Fathi, H., and Rashidi, A. 2011 ‘Progressive 3D reconstruction of infrastructure with videogrammetry’. *Automation in Construction*, Elsevier B.V., 20(7), 884–895.
- El-Omari, S., and Moselhi, O. 2011 ‘Integrating automated data acquisition technologies for progress reporting of construction projects’. *Automation in Construction*, Elsevier B.V., 20(6), 699–705.
- Golparvar-Fard, M., Asce, M., Peña-Mora, F., and Savarese, S. 2011b ‘Integrated Sequential As-Built and As-Planned Representation with D 4 AR Tools in Support of Decision-Making Tasks in the AEC/FM Industry’. *Journal of Construction Engineering and Management*, 137(12), 1099–1116.
- Fathi, H., and Brilakis, I. 2011 ‘Automated sparse 3D point cloud generation of infrastructure using its distinctive visual features’. *Advanced Engineering Informatics*, Elsevier Ltd, 25(4), 760–770.
- Golparvar-Fard, M., Bohn, J., Teizer, J., Savarese, S., and Peña-Mora, F. 2011c ‘Evaluation of image-based modeling and laser scanning accuracy for emerging

- automated performance monitoring techniques'. *Automation in Construction*, Elsevier B.V., 20(8), 1143–1155.
- Powers, D. M. W. 2011 'EVALUATION: FROM PRECISION, RECALL AND F-MEASURE TO ROC, INFORMEDNESS, MARKEDNESS & CORRELATION'. *Journal of Machine Learning Technologies*, 2(1), 37–63.
- Xie, H., Shi, W., and Issa, R. R. A. 2010 'Implementation of BIM /RFID in Computer-Aided Design-Manufacturing- Installation Process'. *IEEE*, 107–111.
- Cheng, T., Yang, J., Teizer, J., and Vela, P. A. 2010 'Automated construction resource location tracking to support the analysis of lean principles'. *Challenging Lean Construction Thinking: What Do We Think and What Do We Know? - 18th Annual Conference of the International Group for Lean Construction, IGLC 18*, 643–653.
- Bosché, F. 2010 'Automated recognition of 3D CAD model objects in laser scans and calculation of as-built dimensions for dimensional compliance control in construction'. *Advanced Engineering Informatics*, Elsevier Ltd, 24(1), 107–118.
- Turkan, Y., Bosche, F., Haas, C. T., and Haas, R. 2010 'Towards Automated Progress Tracking Of Erection Of Concrete Structures'. *Proc. of 6th International AEC Innovation Conference*.
- Hajian, H., and Becerik-Gerber, B. 2010 'Scan to BIM: Factors Affecting Operational and Computational Errors and Productivity Loss'.
- Tang, P., Huber, D., Akinci, B., Lipman, R., and Lytle, A. 2010 'Automatic reconstruction of as-built building information models from laser-scanned point clouds: A review of related techniques'. *Automation in Construction*, Elsevier B.V., 19(7), 829–843.
- Bosche, F., Haas, C. T., and Akinci, B. 2009 'Automated Recognition of 3D CAD Objects in Site Laser Scans for Project 3D Status Visualization and Performance Control'. *Journal of Computing in Civil Engineering*, 23(6), 311–318.
- Golparvar-Fard, M., Peña-Mora, F., and Savarese, S. 2009a 'Monitoring of Construction Performance Using Daily Progress Photograph Logs and 4D As-Planned Models'. *International Workshop on Computing in Civil Engineering 2009*, American Society of Civil Engineers, Reston, VA, 53–63.
- Ibrahim, Y. M., Lukins, T. C., Zhang, X., Trucco, E., and Kaka, A. P. 2009 'Towards automated progress assessment of workpackage components in construction projects using computer vision'. *Advanced Engineering Informatics*, 23(1), 93–103.
- Golparvar-Fard, M., Peña-Mora, F., Arboleda, C. A., and Lee, S. 2009b 'Visualization of Construction Progress Monitoring with 4D Simulation Model Overlaid on Time-Lapsed Photographs'. *Journal of Computing in Civil Engineering*, 23(6), 391–404.
- Zhang, X., Bakis, N., Lukins, T. C., Ibrahim, Y. M., Wu, S., Kagioglou, M., Aouad, G., Kaka, A. P., and Trucco, E. 2009 'Automating progress measurement of construction projects'. *Automation in Construction*, 18(3), 294–301.

- Zhu, Z., and Brilakis, I. 2009 'Comparison of Optical Sensor-Based Spatial Data Collection Techniques for Civil Infrastructure Modeling'. *Journal of Computing in Civil Engineering*, 23(3), 170–177.
- Majid, Z., Setan, H., and Chong, A. K. 2009 'Accuracy Assessments of Point Cloud 3D Registration Method for High Accuracy'. *Geoinformation Science Journal*, 9(2), 36–44.
- Bosche, F., and Haas, C. T. 2008 'Automated retrieval of 3D CAD model objects in construction range images'. *Automation in Construction*, 17(4), 499–512.
- Bosche, F., Haas, C. T., and Murray, P. 2008 'Performance of Automated Project Progress Tracking With 3D Data Fusion'. *Proc. of Congrès annuel 2008 de la SCGC CSCE 2008 Annual Conference*, 1–10.
- Rebolj, D., Babič, N. Č., Magdič, A., Podbreznik, P., and Pšunder, M. 2008 'Automated construction activity monitoring system'. *Advanced Engineering Informatics*, 22(4), 493–503.
- Li, S., Isele, J., and Bretthauer, G. 2008 'Proposed methodology for generation of building information model with laserscanning'. *Tsinghua Science and Technology*, 13(S1), 138–144.
- Navon, R., and Sacks, R. 2007 'Assessing research issues in Automated Project Performance Control (APPC)'. *Automation in Construction*, 16(4), 474–484.
- Chae, S., and Kano, N. 2007 'Application of Location Information by Stereo Camera Images to Project Progress Monitoring'. *Proc. of 24th International Symposium on Automation & Robotics in Construction*, 314–322.
- Akinci, B., Boukamp, F., Gordon, C., Huber, D., Lyons, C., and Park, K. 2006 'A formalism for utilization of sensor systems and integrated project models for active construction quality control'. *Automation in Construction*, 15(2), 124–138.
- Remondino, Fabio; El-Hakim, S. 2006 'Image-based 3D modelling: A review'. *Photogrammetric Record*, Blackwell Publishing Ltd, 21(115), 269–291.
- Li, H., Chen, Z., Yong, L., and Kong, S. C. W. 2005 'Application of integrated GPS and GIS technology for reducing construction waste and improving construction efficiency'. *Automation in Construction*, 14(3), 323–331.
- Tissainayagam, P., and Suter, D. 2005 'Object tracking in image sequences using point features'. *Pattern Recognition*, 38(1), 105–113.
- Navon, R. 2005 'Automated project performance control of construction projects'. *Automation in Construction*, 14(4), 467–476.
- Sternberg, H., Jahn, I., Kinzel, R., Techniques, M., Heritage, C., and Schwartau, B. 2004 'Terrestrial 3D Laser Scanning – Data Acquisition and Object Modelling for Industrial As-Built Documentation and Architectural Applications'. XXXV(July), 942–947.
- Serby, D., Meier, E. K., and Van Gool, L. 2004 'Probabilistic object tracking using

multiple features'. *Proceedings of the 17th International Conference on Pattern Recognition, 2004. ICPR 2004.*, 184–187 Vol.2.

Sacks, R., Akinci, B., and Ergen, E. 2003 '3D modeling and real-time monitoring in support of lean production of engineered-to-order precast concrete buildings'. *Journal of the International Group for Lean Construction*.

Cheng, M. Y., and Chen, J. C. 2002 'Integrating barcode and GIS for monitoring construction progress'. *Automation in Construction*, 11(1), 23–33.

Graves, S., and Burner, A. 2001 'Development of an intelligent videogrammetric wind tunnel measurement system'. *Proc. of International Symposium on Optical Science and Technology*.

Triggs, B., McLauchlan, P. F., Hartley, R. I., and Fitzgibbon, A. W. 2000 'Bundle Adjustment — A Modern Synthesis'. *Vision Algorithms: Theory and Practice*, 298–372.

Stehman, S. V. 1997 'Selecting and Interpreting Measures of Thematic Classification Accuracy'. *Remote Sensing of Environment*, 62(1), 77–89.

Horn, B. K. P. 1987 'Closed-form solution of absolute orientation using unit quaternions'. *Journal of the Optical Society of America A*, 4(4), 629–642.

APPENDIX

C++ Prototype of the Automated Progress Recognition System

```
//Common Headers
#include <iostream>
#include <vector>
#include <pcl/common/common.h>
//Point cloud io headers
#include <pcl/io/obj_io.h>
#include <pcl/io/pcd_io.h>
#include <pcl/io/ply_io.h>
#include <pcl/point_types.h>
//PCL visualization headers
#include <pcl/visualization/pcl_visualizer.h>
#include <pcl/visualization/cloud_viewer.h>
//PCL Segmentation Headers
#include <pcl/search/search.h>
#include <pcl/search/kdtree.h>
#include <pcl/features/normal_3d.h>
#include <pcl/filters/passthrough.h>
#include <pcl/segmentation/region_growing.h>

typedef struct
{
    float x;//Struct for storing points
    float y;
    float z;
} point3D;
point3D grid[60][60][60]={0};// 3D array of points referenced by ijk

struct voxel
{//Structure Voxel→store each voxel information
```

```

    point3D points[9]; //Stores the 8 vertices of a voxel
float xmin, xmax, ymin, ymax, zmin, zmax; //Stores min & max of x,y,z of a voxel
int count; //Stores no. of points present inside a voxel
bool clasf; //Binary classifier → determines 'BUILT'/'NOT BUILT'
};
voxel vox[60][60][60];
voxel bim[60][60][60]={0};

```

```

//function to calculate max limits of triangle

```

```

float findmax(float a, float b, float c)

```

```

{
float maxi = a;
if(b > maxi)
{
    maxi = b;
}
if(c > maxi)
{
    maxi = c;
}
return(maxi);
}

```

```

//Function to calculate the min limits of triangle

```

```

float findmin(float a, float b, float c)

```

```

{
float mini = a;
if(b < mini)
{
    mini = b;
}
if(c < mini)
{
    mini = c;
}
}

```

```

}
return(mini);
}

//CALCULATE THE MIN AND MAX OF EACH VOXEL
void calculate_minmax(int i,int j,int k)
{
//Initialize the min and max values to the first element
vox[i][j][k].xmin = vox[i][j][k].xmax = vox[i][j][k].points[1].x;
vox[i][j][k].ymin = vox[i][j][k].ymax = vox[i][j][k].points[1].y;
vox[i][j][k].zmin = vox[i][j][k].zmax = vox[i][j][k].points[1].z;

for(int v =1; v <=8; v++)
{
if(vox[i][j][k].points[v].x < vox[i][j][k].xmin)
{
vox[i][j][k].xmin = vox[i][j][k].points[v].x;
}
if(vox[i][j][k].points[v].x > vox[i][j][k].xmax)
{
vox[i][j][k].xmax = vox[i][j][k].points[v].x;
}
}
for(int v =1; v <=8; v++)
{
if(vox[i][j][k].points[v].y < vox[i][j][k].ymin)
{
vox[i][j][k].ymin = vox[i][j][k].points[v].y;
}
if(vox[i][j][k].points[v].y > vox[i][j][k].ymax)
{
vox[i][j][k].ymax = vox[i][j][k].points[v].y;
}
}
}
}

```

```

for(int v =1; v <=8; v++)
{
if(vox[i][j][k].points[v].z < vox[i][j][k].zmin)
{
    vox[i][j][k].zmin = vox[i][j][k].points[v].z;
}
if(vox[i][j][k].points[v].z > vox[i][j][k].zmax)
{
    vox[i][j][k].zmax = vox[i][j][k].points[v].z;
}
}

cout <<"xmin: " << vox[i][j][k].xmin <<"xmax:" << vox[i][j][k].xmax <<"\n";
cout <<"ymin: " << vox[i][j][k].ymin <<"ymax:" << vox[i][j][k].ymax <<"\n";
cout <<"zmin: " << vox[i][j][k].zmin <<"zmax:" << vox[i][j][k].zmax <<"\n";
}

pcl::PointCloud<pcl::PointXYZ>::Ptr cloud_cluster(new
pcl::PointCloud<pcl::PointXYZ>);//Global variable
int no_segments =0;

int notu =0, notf =0;
void binaryclassifier(int i,int j,int k,int threshold,const
pcl::PointCloud<pcl::PointXYZ>::ConstPtr &input1)
{
float xval, yval, zval;

int coo = input1->points.size();
    vox[i][j][k].count =0;
for(size_t v =0; v <= coo -1; v++)
{
    xval = input1->points[v].x;    yval = input1->points[v].y;    zval = input1->
points[v].z;

```

```

if((xval >= vox[i][j][k].xmin)&&(xval <= vox[i][j][k].xmax))&&((yval >=
vox[i][j][k].ymin)&&(yval <= vox[i][j][k].ymax))&&((zval >=
vox[i][j][k].zmin)&&(zval <= vox[i][j][k].zmax)))
    vox[i][j][k].count++;
}
if(vox[i][j][k].count >= threshold)
{
    vox[i][j][k].clasf =true;
    std::cout <<"no.of points in vox["<< i <<"]["<< j <<"]["<< k <<"] is: "<<
vox[i][j][k].count <<"\n";
    notu = notu +1;
}
else
{
    vox[i][j][k].clasf =false;
    notf = notf +1;
}
}
void binaryclassifier_BIM(int i,int j,int k,int threshold,const
pcl::PointCloud<pcl::PointXYZ>::ConstPtr &input2)
{
    float xval, yval, zval;

    int coo = input2->points.size();
    for(size_t v =0; v <= coo -1; v++)
    {
        xval = input2->points[v].x;    yval = input2->points[v].y;    zval = input2-
>points[v].z;
        if((xval >= vox[i][j][k].xmin)&&(xval <= vox[i][j][k].xmax))&&((yval >=
vox[i][j][k].ymin)&&(yval <= vox[i][j][k].ymax))&&((zval >=
vox[i][j][k].zmin)&&(zval <= vox[i][j][k].zmax)))
            bim[i][j][k].count++;
    }
    if(bim[i][j][k].count >= threshold)
    {
        bim[i][j][k].clasf =true;

```

```

        notu = notu +1;
    }
else
{
    bim[i][j][k].clasf =false;
    notf = notf +1;
}
}

int main()
{
    std::string bfilename, ptclfilename;

    std::cout <<"enter BIM file name\n";
    std::cin >> bfilename;
    std::cout <<"enter pointcloud file name\n";
    std::cin >> ptclfilename;
//load the BIM point cloud
    pcl::PointCloud<pcl::PointXYZ>::Ptr bim_cloud(new
pcl::PointCloud<pcl::PointXYZ>);
    if(pcl::io::loadOBJFile(bfilename,*bim_cloud)==-1){ std::cout <<"Cannot load BIM
file \n";return(-1);}

//Load the scan point cloud file
    pcl::PointCloud<pcl::PointXYZ>::Ptr scan(new
pcl::PointCloud<pcl::PointXYZ>);
    if(pcl::io::loadOBJFile(ptclfilename,*scan)==-1){ std::cout <<"Cannot load the
point zed file\n";return(-1);}

//Autodetect which threshold to use for supplied fiel (ZED or Tango)
int filetype1, filetype2, threshold;

    std::string z("z");
    if(ptclfilename.compare(0, z.length(), z)==0)

```



```

{
    threshold =40;//threshold =1 for site
}
else
{
    threshold =250;//threshold =1 for site
}
std::cout <<"threshold: " << threshold <<"\n";

//get minimum and maxim x and y values from cluster 1 file
float Max_x, Min_x, Max_y, Min_y, Min_z, Max_z;
Eigen::Vector4f modelMin = Eigen::Vector4f::Zero(); Eigen::Vector4f modelMax
= Eigen::Vector4f::Zero();
pcl::getMinMax3D(*bim_cloud, modelMin, modelMax);

int TP =0, TN =0, FP =0, FN =0;

int userinput;
std::cout <<"Enter the plane for generating the point cloud\n";
std::cout <<" XY --- 1\n";
std::cout <<" YZ --- 2\n";
std::cout <<" ZX --- 3\n";
std::cout <<" BIM -- 4\n";
cin >> userinput;

float Xe, Xs, Ye, Ys, Ze, Zs;
Xe = modelMax[0]; Xs = modelMin[0];
Ye = modelMax[1]; Ys = modelMin[1];
Ze = modelMax[2]; Zs = modelMin[2];

//Compute edge sizes of whole file
float x_size = abs(Xe - Xs);
float y_size = abs(Ye - Ys);
float z_size = abs(Ze - Zs);

```

```

//Specify steps (edge length of each voxel)
float x_step =0.11;
float y_step =0.11;
float z_step =0.11;

//compute the no. of points to be generated in each axis
float n_stepx =(int)((x_size / x_step)+0.5);
float n_stepy =(int)((y_size / y_step)+0.5);
float n_stepz =(int)((z_size / z_step)+0.5);
    point3D p;

//Points per edge (including ending point)
int n1 = n_stepx +1;
int n2 = n_stepy +1;
int n3 = n_stepz +1;
int a, b, c;//a is for i. b is j. c is k
int r, s, t;

switch(userinput)
{
case1:// if XY plane
    a = n1;   r =1;
    b = n2;   s =1;
    c =2;     t =1;
break;
case2://YZ plane
    a =2;     r =1;
    b = n2;   s =1;
    c = n3;   t =1;
break;
case3://ZX plane
    a = n1;   r =1;
    b =2;     s =1;
    c = n3;   t =1;

```

```

break;
case4:
    a = n1;   r = 1;
    b = n2;   s = 1;
    c = n3;   t = 1;
break;
}
//Generate the equally spaced points based on BIM file
for(int i = 0; i < a; i++)
{
//move on x axis
for(int j = 0; j < b; j++)
{
//move on y axis
for(int k = 0; k < c; k++)
{
//move on z axis
    p = {0};
    p.x = Xs +(x_step * i);
    p.y = Ys +(y_step * j);
    p.z = Zs +(z_step * k);
    grid[i][j][k]= p;
    cout << i << j << k << " " << p.x << " " << p.y << " " << p.z << "\n";
}
}
}

for(int i = 0; i < a - r; i++)
{
//move on x axis
for(int j = 0; j < b - s; j++)
{
//move on y axis
for(int k = 0; k < c - t; k++)
{
//move on z axis
    vox[i][j][k].points[1]= grid[i][j][k];
    vox[i][j][k].points[2]= grid[i + 1][j][k];
    vox[i][j][k].points[3]= grid[i][j + 1][k];
    vox[i][j][k].points[4]= grid[i + 1][j + 1][k];
}
}
}

```

```

vox[i][j][k].points[5]= grid[i][j][k + 1];
vox[i][j][k].points[6]= grid[i + 1][j][k + 1];
vox[i][j][k].points[7]= grid[i][j + 1][k + 1];
vox[i][j][k].points[8]= grid[i + 1][j + 1][k + 1];

//Calculate the min and max value of x y z for visualization function for each voxel
calculate_minmax(i, j, k);

//Check if points in the scan are inside the voxel
binaryclassifier(i, j, k, threshold, scan);
int bthreshold =13;//threshold =1 for site
binaryclassifier_BIM(i, j, k, bthreshold, bim_cloud);
if((vox[i][j][k].clasf ==true)&&(bim[i][j][k].clasf ==true))
    TP++;
if((vox[i][j][k].clasf ==false)&&(bim[i][j][k].clasf ==false))
    TN++;
if((vox[i][j][k].clasf ==false)&&(bim[i][j][k].clasf ==true))
    FN++;
if((vox[i][j][k].clasf ==true)&&(bim[i][j][k].clasf ==false))
    FP++;
}
}
}

//view the voxel and the points inside it
pcl::visualization::PCLVisualizer view;
std::stringstream ss;

view.addPointCloud(bim_cloud);
for(int i =0; i < a - r; i++)
{//move on x axis
for(int j =0; j < b - s; j++)
{//move on y axis
for(int k =0; k < c - t; k++)
{//move on z axis

```

```

        std::cout << "[" << i << "]" "[" << j << "]" "[" << k << "]" " << vox[i][j][k].clasf << "
" << bim[i][j][k].clasf << " " << vox[i][j][k].count << " " << bim[i][j][k].count << "\n";
        ss << "cube" << i << j << k;
if(vox[i][j][k].clasf && bim[i][j][k].clasf)
        view.addCube(vox[i][j][k].xmin, vox[i][j][k].xmax, vox[i][j][k].ymin,
vox[i][j][k].ymax, vox[i][j][k].zmin, vox[i][j][k].zmax, 0, 128, 0, ss.str(), 0);
else
        view.addCube(vox[i][j][k].xmin, vox[i][j][k].xmax, vox[i][j][k].ymin,
vox[i][j][k].ymax, vox[i][j][k].zmin, vox[i][j][k].zmax, 1.0, 0, 0, ss.str(), 0);
    }
}
}
//view.setRepresentationToWireframeForAllActors();
view.addCoordinateSystem(1.0);
while(!view.wasStopped())
    view.spinOnce();

//DISPLAY THE ACCURACY OF PROGERSS MEASURED
    std::cout << "TP: " << TP << " TN: " << TN << " FP: " << FP << " FN: " << FN
<< "\n";
return(0);
}

```

CURRICULUM VITAE

Name : MADHUMITHA SENTHILVEL
Date of Birth : 21-04-1992
Educational Qualification : Bachelor of Technology (Hons.), 2013
Institution : SASTRA University, Thanjavur
Specialization : Civil Engineering

GENERAL TEST COMMITTEE

CHAIR PERSON:

Dr. K. Ananthanarayan

Professor

Department of Civil Engineering

GUIDE:

Dr. Koshy Varghese

Professor

Department of Civil Engineering

Dr. Ramesh Babu

Professor

Department of Mechanical Engineering

MEMBERS:

Dr. Palaniappan Ramu

Professor

Department of Engineering Design

Dr. Benny Raphael

Associate Professor

Department of Civil Engineering

This is to certify that the thesis titled '**AUTOMATED CONSTRUCTION MONITORING USING RANGE IMAGING**', submitted by **Madhumitha Senthilvel**, to the Indian Institute of Technology Madras, for the award of the degree of Master of Science, is a bonafide record of the research work carried out by her under my supervision. The contents of this thesis, in full or in parts, have not been submitted to any other Institute or University for the award of any degree or diploma.